Biosynthesized Selenium co-catalyst for Improved Photocatalytic activity of Se-ZnO Nanocomposites

A Dissertation

Submitted in the partial fulfillment of requirement for the award of the Degree of

Master of Science
In
Biochemistry

Submitted by

Alisha Vaishnav (301607003)

Under the supervision of

Dr. Bonamali Pal
Professor
School of Chemistry and Biochemistry

Dr. N. Tejo Prakash
Professor & Associate Dean
School of Energy and Environment

School of Chemistry and Biochemistry Thapar Institute of Engineering & Technology
Patiala-147004 Punjab, India

July, 2018

Certificate

I hereby certify that the work presented in this thesis entitled "**Biosynthesized Selenium co-catalyst for Improved Photocatalytic activity of Se-ZnO Nanocomposites**" submitted in partial fulfillment of the requirements for the award of degree of Master of Science in Biochemistry submitted to School of Chemistry and Biochemistry, Thapar Institute of Engineering and Technology, Patiala is an authentic record of my own work carried out under the supervision of Dr. Bonamali Pal and Dr. N. Tejo Prakash. The matter embodied in the thesis has not been submitted to any other University for the award of any other degree or diploma. Works of other authors cited in this thesis have been duly acknowledged under reference section of this thesis.

Alisha Vaishnav

Date: **Alisha Vaishnav**

This is to certify that the above statement made by the candidate is correct and true to the best of our knowledge.

Dr. Bonamali Pal Professor
School of Chemistry & Biochemistry Thapar Institute of Engineering & Technology, Patiala-147001

Dr. N. Tejo Prakash Professor & Associate Dean
School of Energy & Environment Thapar Institute of Engineering & Technology, Patiala-14700

Acknowledgements

Through this section of the thesis, I would like to convey my heartiest thanks to all those who supported and encouraged me in many ways throughout for the accomplishment of this project.

I would like to extend my sincerest gratitude to my supervisor Dr. Bonamali Pal Professor, School of Chemistry and Biochemistry, Thapar Institute of Engineering and Technology, Patiala for giving me the valuable opportunity to work under his worthy guidance. He has been a source of inspiration and direction to me. It was his splendid supervision, support and unending patience that helped me in executing this task from its conception to completion.

I take this opportunity to thank to my Co- Supervisor Dr. N. Tejo Prakash, Professor and Associate Dean, School of Energy & Environment, Thapar Institute of Engineering and Technology, Patiala for helping me with his immense knowledge, Constructive ideas, critical and timely suggestions, effort, time and patience throughout my work.

I would also like to acknowledge faculty of School of chemistry and Biochemistry, Thapar Institute of Engineering and Technology, Patiala for their encouraging and supporting nature and specially Dr. Amjad Ali, Head, School of Chemistry and Biochemistry, Thapar Institute of Engineering and Technology, Patiala for allowing me to work on the project of my choice. I am also grateful to other staff members of school of Chemistry and Biochemistry.

Special thanks to Miss Himadri, Mr. Rahil Changotra, Mr. Sumit Jaiswal and Miss Tanushree for their kind assistance, cooperation and generous help whenever I needed. I have deep gratitude towards them never and never turning down any query. I would also like to thank Mr. Adil Bhatla for their timely help, support and encouragement.

I would like to express my regards to my family for being source of inspiration, dedication and encouragement in my life.

Finally, praises and thanks to the almighty God, the most merciful and compassionate, for His blessings throughout my project work to complete it successfully.

Date:

Alisha Vaishnav

Table of Contents

List of Abbreviations

TSB	Tryptone Soya Broth
TSA	Tryptone Soya Agar
CB	Conductance band
VB	Valence band
UV-Vis	Ultraviolet-Visible
Wt %	Weight percent
DRS	Diffuse reflectance spectrophotometer
DLS	Dynamic Light scattering
SEM	Scanning electron microscope
EDX	Energy dispersive X-ray
HR-TEM	High Resolution Transmission Electron Microscope
XRD	X-Ray Diffraction
Se@ZnO	Selenium doped Zinc Oxide
NPs	Nanoparticles
Pd	Palladium
Pt	Platinum
Au	Gold
sp.	Species
Se- NPs	Selenium nanoparticles
4-CG	4-Cholоguaiacol

List of Symbols

K	Rate Constant
M	Molarity
Mg	Milli gram
mM	Milli molar
mL	Milli liter
g	Gram
L	Liter
N	Normality
nm	Nano meter
ng	Nano gram
rpm	Revolutions per minute
µL	Micro liter
$\mathbf{e^-}$	Electron
$\mathbf{h^+}$	Hole
min	Minute
eV	Electron Volt
a.u.	Arbitrary unit
$\boldsymbol{\lambda_{max}}$	Maximum wavelength
$\mathbf{E_g}$	Energy Gap
ppm	Parts Per Million

List of Schemes

Abstract

The present study deals with the biosynthesis of selenium nanoparticles and their impregnation as co-catalyst on ZnO semiconductor. The synthesized catalyst was characterized for its physicochemical properties using UV-DRS, DLS, TEM, SEM-EDS and XRD. The potential of biosynthesized catalyst was tested against the photocatalytic degradation of recalcitrant compound 4-chloroguaiacol and real pharmaceutical industry effluent. Various concentrations of Se were doped on ZnO semiconductor and 0.5wt% was found to be the most optimum. Effect of Photocatalyst on different concentrations of model compound was also evaluated. Photocatalytic reactions were carried out using solar radiations to make the process cost effective. Kinetic study of degradation reaction was performed and it was observed to follow first-order reaction kinetics. Complete mineralization of model compound was confirmed when 88% of CO_2 evolution was observed at the completion of the reaction. The potential of biosynthesized catalyst was also assessed against the treatment of real pharmaceutical industrial effluent and significant COD reduction of 50% was observed.

1. INTRODUCTION

From the past few years nanotechnology has proven itself as a promising and powerful tool for scientific research innovations. Due to unique catalytic, optical, electronic and magnetic properties[1], nanoparticles synthesized using metals have their implementation in various fields like electronics, medicine and in several industries [2-4]. Zinc oxide (ZnO) is considered as one of the most promising Photocatalyst for the degradation of organic pollutants and detoxification of water[5]. Its significant activity is attributed to its unique characteristics such as high number of active sites and surface area[6], direct and wide band gap in the near-UV spectral region [7], strong oxidation ability, good photocatalytic property, and a large free-exciton binding energy [8]. ZnO nanoparticles have also shown their potential as antimicrobial agents. In semiconductor particles where electron/hole (e^-/h^+) recombination rate is too fast, it results in the decreased quantum yield of photocatalytic processes [9]and also causes wastage of energy. Therefore, for the efficient photocatalysis, (e^-/h^+) recombination process should be inhibited. Metal doping enhances the charge separation between electrons and holes, and hence, counters the recombination process. Doping of metal ions on ZnO can positively influence the photocatalytic performance of semiconductor material. Nanomaterial co-catalysts play an important role in the improvement of photocatalysts activity. When semiconductor NPs come in contact with co-catalyst (metal/non- metal/semiconductor), fermi-level/energy band equilibrium occurs. The electrons can be easily trapped by noble metals such as Pd, Pt, and Au because of their low fermi levels. However, the practical application of noble metals as co-catalyst is inhibited due to their cost and scarcity. Hence, formulation of efficient and relatively low cost co-catalyst is important.

In this context, Se doping was performed in order to increase the separation of charged carriers and to further extend the optical properties of ZnO in visible region so that the solar energy can be used for practical applications. In the present study, biologically synthesized Selenium doped ZnO NPs were utilized and assessed for their photocatalytic potential as shown in scheme 1. Selenium was selected as a dopant due to its suitable chemical and biological properties and ease of synthesis of Se-ZnO nanoparticles. Se is expected to facilitate the formation of reactive oxygen species (ROS) like hydroxyl radicals (˙OH) due to its high reduction potential which is considered as favorable for the transfer of photo generated electrons from conduction band to valance band[10]. Selenium possess properties such as narrow band gap (1.7-2 eV), high refractive index, relatively low melting point i.e. ~217°C and high reactivity which makes it suitable for performing oxidation reactions[11-12].

Previous research demonstrated that Se nanoparticles (Se NPs) exhibit significant photocatalytic potential against the degradation of Congo red and methylene blue dye under UV irradiation[13-14]. Se-NPs are known for their significant applications in photoconductivity, photo degradation and treatment of wastewater. Also, biosynthesis of Se nanoparticles has been performed with different bacterial species [15]. The formation of Se NPs is initiated by the reduction of selenate/selenite oxyanions to form elemental selenium (Se^o) which is non-toxic and insoluble in water [16]. Different types of bacteria existing in aquatic and terrestrial environments, in both Se-rich and Se-free soils have the potential to reduce selenate/selenite oxyanions to non-toxic forms [17-18].

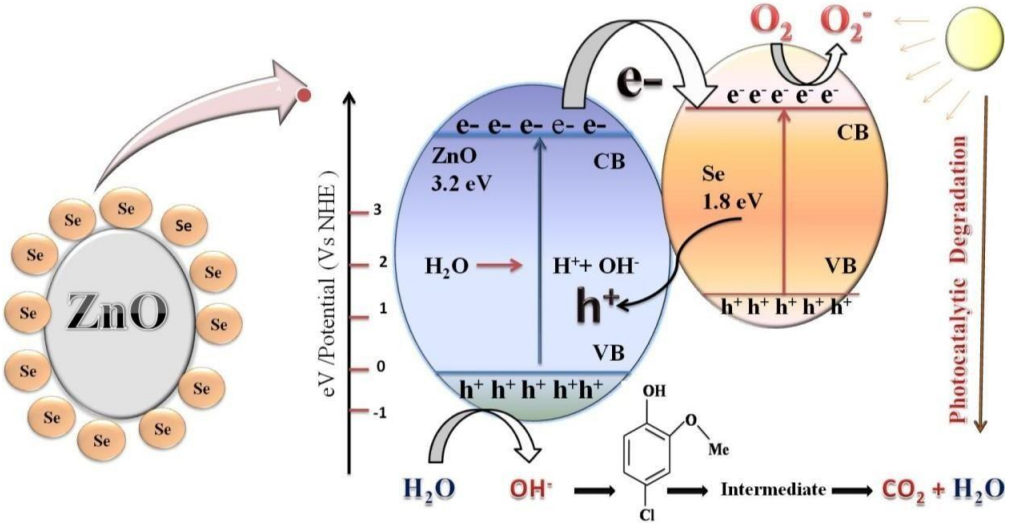

Scheme 1: Scheme representing the photocatalytic application of Se doped ZnO nanoparticles under sunlight irradiation.

The conventional physical and chemical synthesis approaches are successful but have some limitations which are hazardous, tedious and environmentally challenging [19]. Therefore, it is a need of time to develop and study eco-friendly nanomaterials synthesis procedures. Nanoparticle synthesis by biological means is fetching great attention as this approach utilizes living cells and hence consider as "green" approach [20-22]. The advantages associated with biological synthesis approach are relatively low cost, elimination of intense processing conditions through the feasible synthesis at physiological temperature, pH and less synthesis time. In this area, prokaryotic bacteria have gained consideration due to its genetic manipulation and handling ease [23].

4-Chloroguaiacol (4-CG) is a widespread recalcitrant pollutant present in pulp and paper effluents [19]. Softwood pulp effluents contain abundant amount of chlorinated derivatives like catechol, vanillin, phenol and guaiacol [24]. The problems associated with these

compounds are their carcinogenic and mutagenic impacts on environment, resistance to biodegradation, toxicity, drinking water pollution, adverse impacts on human respiratory and nervous system like altered pulmonary function and chronic bronchitis [25]. Most of the chlorophenolic compounds are present on priority organic pollutants list by the US-Environmental Protection Agency. Various treatment methods have been employed for their removal from aqueous solutions, including biological treatment, reverse osmosis, catalytic wet oxidation, adsorption, electrochemical degradation, photocatalysis and ionizing radiations. Due to the extensive use of these compounds and their derivatives in industries like pesticide, petroleum, solvent, paint and pharmaceutical production [26], their effluents need specialized treatment before being dispensed into water stream. So, 4-CG was selected as model compound. Photocatalytic degradation of real pharmaceutical effluent was also performed to check the practical applicability of synthesized Se@ZnO NPs for the treatment of real wastewater. The efficiency of catalyst was evaluated in terms of reduction in chemical oxygen demand (COD).

2. Objectives

- Biosynthesis of extracellular selenium (Se) nanoparticles.
- Synthesis of Se@ZnO nanocomposites using different weight percent Se as co-catalyst.
- Enhanced photocatalytic activity of Se@ZnO nanocomposite for degradation of pollutant 4-chloroguaiacol and real pharmaceutical effluent

3. Experimental Section

3.1 Chemical Reagents

Tryptone soya broth (TSB) and Tryptone soya agar (TSA) were purchased from Hi-media, India. Sodium selenate (Na_2SeO_4), absolute ethanol, acetone were obtained from Sigma Aldrich, India. Zinc oxide (ZnO), 4-Choro Guaiacol (ClC_6H_3 (OCH_3), was purchased from Loba Chemie, India. The bacterial strain used in the study, Bacillus sp., was isolated from selenium- rich soil of Punjab region. All the chemicals and culture media used in the present study were of analytical grade and used without further purification. Double distilled water was obtained using ultra filtration system (Mili-Q, Millipore)

3.2 Methods

3.2.1. Isolation of selenium tolerant bacteria

Se tolerant bacterial isolates were isolated from soil sample collected from Se-affected agricultural land geographically located at 31˚13′N, 76˚21′E, in the Jainpur village of Nawanshahar district, Punjab (India). 1 g soil sample was inoculated into 250 ml Erlenmeyer flask containing 100 ml sterile Trypton Soya Broth (TSB) and incubated at 37° C, 120 rpm for 24 h. After serial dilutions (10^{-5}-10^{-6} times) with sterile saline, 100 µl of bacterial suspension was spread aseptically over petri dish (90 mm) containing Trypton Soya Agar (TSA) medium supplemented with 5 mM Se (as Sodium selenate). Plate was further incubated at 37° C for 48h. Bacteria having selenate ion reducing capability formed visually distinct red or orange-red colonies. Change in colony color was observed due to enzymatic reduction of selenate ion into red color, amorphous, elemental selenium nanoparticles (Se-NPs).

3.2.2. Biosynthesis and isolation of extracellular Se nanoparticles

Different colonies grown on 5 mM Se rich TSA plate were randomly selected and inoculated separately in culture tubes containing 5 ml TSB enriched with 10 mM Se. The tubes were further inoculated at 37° C, 120 rpm for 48 h. For the screening bacterial strain producing extracellular Se NP, 1 ml culture broth from each tube were transferred into 1.5 ml microfuge tube and centrifuged at 5000 rpm for 10 min. After centrifugation, the cell free supernatants having Orange-red color confirmed the presence of extracellular Se NPs. Pure culture of bacterial strain producing smaller particle size was maintained and further used for the mass production of Se NPs. For the isolation of extracellular Se NPs, 4 days grown culture broth was centrifuged at 5000 rpm for 10 min. The supernatant containing Se NPs was centrifuged at 10,000 rpm for 10 min. The obtained Se NP pellet was further washed 3 times and stored as suspension in distilled water at 4° C.

3.2.3. Quantification of Selenium Nanoparticles

The amount of Se in the NPs solution obtained from bacteria was quantified by the microwave acid digestion method. The digestion process was carried out in two steps, Firstly, 20 µl of Se NPs were digested with 5ml of 3:1 solution of nitric and perchloric acid (HNO_3 + $HCLO_4$) and kept in microwave digester (MARS 6, CHEM) for 30 min for 180˚C and in second step 5ml ,6 M HCl is added to the digester tubes, for 30 min at 150˚C.Thereafter , the

digested samples were cooled and transferred to a volumetric flask and final volume was made upto 20ml with 0.1N HCl. Futherrmore,100 µL of the digest was taken in a tube containing 12.5 M formic acid and 0.04M stabilizing agent (0.04M solution of Na_2EDTA in 10% hydroxylamine hydrochloride). The pH of the digested solution was adjusted to 1.8 with 4.0N NH_4OH, the digest was incubated for 10 min at 50˚C. For Se analysis, 500 µL of DAN solution was added to derivate the mixture, followed by incubation in water bath at 50˚C for 30min, Finally the reaction mixture was cooled and 3.0ml of cyclohexane and was added to each tube. The reaction between diamines and selenite produce a fluorescent compound, piazselenol which was measured using fluorescence spectrometer (Perkin Elmer LS-45, UK) at excitation and emission wavelength of 360 and 520 nm. The relative method was done using emission Spectrum of National Institute of Standards and Technology (NIST) certified Se-ICP standard solution (SRM-1349) (2-10 ng/mL) was followed to quantify Se [27].

3.2.4. Synthesis of Se Impregnated ZnO nanocomposites (Se@ZnO NCs)

Se@ZnO nanocomposites have been synthesized by wet Impregnation method shown in scheme 2 followed by calcination as reported previously [28]. 200 mg commercially available ZnO was mixed with 10 ml of distilled water under continuous stirring for 2 h. Different volume of Se NPs suspension (5mg/ml) were added dropwise to the ZnO solution and kept for overnight stirring at 1200 rpm. The Se@ZnO nanocomposites was recovered through centrifugation (5000 rpm, 5min) and further washed three times with distilled water. The nanocomposites was dried at 80˚C in hot air oven for 1 hour and crushed into fine powder using motor and pestle. The powder obtained was further sintered in muffle furnace at 200˚C for 2 h. Different w% Se doped ZnO catalyst were prepared by varying the amount of Se NPs (100µl to 400µl).

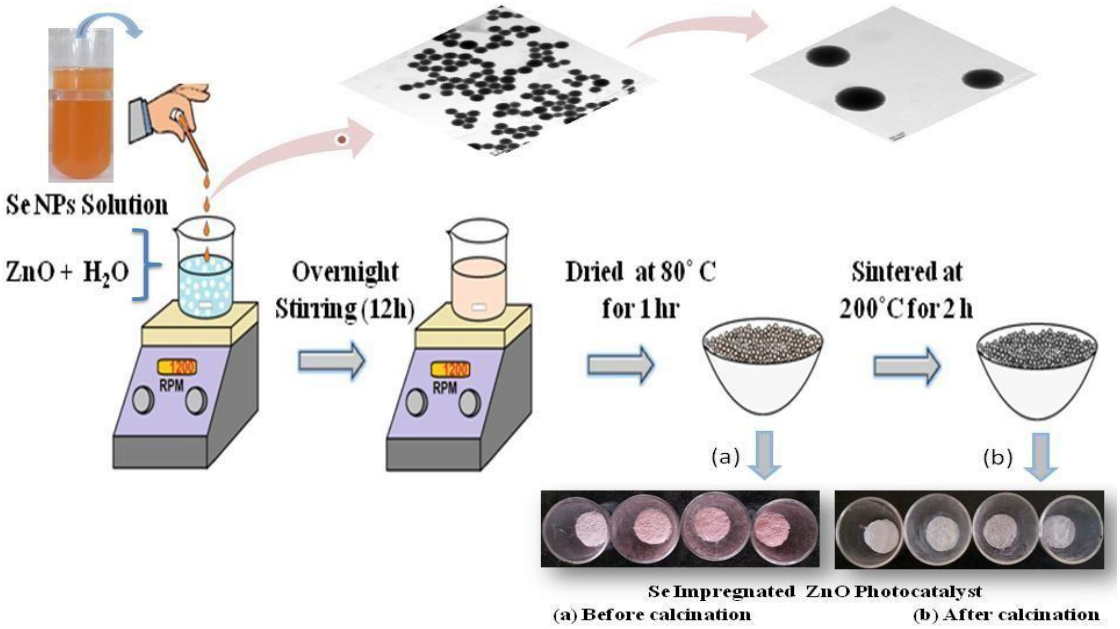

Scheme 2: Scheme representing the formation of Se impregnated ZnO nanocomposites with varying wt% of Se.

3.2.5. Photo degradation of 4-chloroguaiacol and Pharmaceutical Real Effluent

20ppm 4-CG was treated with 5mg/5ml, ZnO and Se@ZnO was used to study the enhanced degradation activity of Se impregrenated ZnO Photocatalyst. The ZnO and different wt % Se doped Photocatalyst was weighed and dissolved in 20 ppm 4CG solution .The reaction tubes were kept under solar radiation with intensity of 791±20 Wm^2 , 39˚C±2˚C for 15mins with continuous stirring. Further reaction was studied with 50 ml -50ppm 4CG.The supernatant was filtered with 0.45 µm polycarbonate filter and absorbance of the supernatant was measured by scanning the sample between the range 200-700 nm in the UV-Visible spectrophotometer.

Similarly, the pharmaceutical real effluent sample with initial COD mg of 1050 mgL^{-1} was taken from a drug manufacturing industry, parabolic drugs limited located in Derabassi, Punjab. The beaker containing 19.76 mL of real effluent was completed with 0.24 mL water. The Photocatalytic activity was measured by COD was values. Chemical oxygen demand (COD) analysis was done by closed reflux method as described in Standard APHA methods (1989) [29].

3.2.6. Characterization Techniques

UV- Visible Spectroscopy

UV- Visible Spectroscopy is used for identification and characterization of nanoparticles. The reduction in beam of light after it passes through the sample is measured by UV-Vis spectrophotometer. Absorption spectra provides the information about size distribution ,band gap and nanoparticles formation as the NPs have unique optical properties that are sensitive to size, shape, concentration, agglomeration state, and refractive index near the nanoparticle surface. Analysis has been done on Hitachi V- 500 UV VIS- Japan double bean spectrophotometer. 800 µl of NPs solution was taken in 1 ml quartz cuvette in the detection range of 190-1100 nm and the baseline was set with double distilled water. ZnO has direct and wide band gap 3.3 eV at room temperature [30]

Dynamic light scattering (DLS)

This technique is used to measure the size of the particles in sub micron region. The particles in suspension undergo the Brownian motion due to the bombardment between the particles and solvent molecules.DLS measures Brownian motion and relates this to the size of the particles. Due to changing constructive/destructive interference of scattered light, random fluctuations occur, which ultimately leads to random motion. The larger the particle, the slower the Brownian motion will be. For analysis, sample was sonicated for 30 min and further 1.5ml aqueous solution of NPs was taken in a cuvette.

X-Ray Diffraction (XRD) Analysis

Powder X-Ray diffraction is a versatile, non destructive analytical technique primarily used for the identification of crystalline phases of molecules, quantitative phase analysis and determination of unit cell dimensions and elucidates three dimensional atomic structure of crystalline solid. Bragg's law calculates the angle where constructive interference from X-rays scattered by parallel planes of atoms will produce a diffraction peak. The XRD pattern analysis was done by Panalytical's X'Pert Pro diffractrometer that consists of vertical theta-theta goniometry having range of 0-1600 2θ K-alpha-1(k = 1.5060A˚) Cu K radiation was used where as nickel metal is used as beta filter.

A smooth surface was used to press the powder a sample into a sample holder.XRD study was done from sophisticated Analysis Instrumentation Laboratory (SAI Lab), Punjab University, Chandigarh, India.

Scanning Electron Microscopy (SEM)

This microscopy technique reveals the information about external morphology, chemical composition, topography, crystallographic information about the surface of sample. For bacterial samples, single colony of bacteria was taken from the TSA plates without Se dose and TSA plates supplemented with Se. Bacterial cells with supplemented Se were filtered through polycarbonate micropores filters (0.22µm), followed by three times washing with Tris–HCl buffer (pH-8.0). The fixation process was carried out with 3% gluteraldehyde in 0.1 M phosphate buffer (pH 7.4) for 60 min. The suspension was centrifuged at 10,000g for 10 min at 4˚C. The pellet obtained, was three times washed with Tris–HCl buffer and then by deionized water [29]. The samples were dehydrated with 70% ethyl alcohol and dried for 30 minutes. Sample of Se-ZnO nanocomposites was prepared by mixing 1mg of nanocomposites with 70 of ethanol and finally sample was sonicated for 1 hr. Both the samples were mounted on an Au coated specimen stub and visualized under SEM JSM-7600F (0.1-30 KV).

Energy Dispersive X-Ray (EDX) spectroscopy

It is an X-ray micro analytical technique that gives qualitative and quantitative information on the chemical composition and elemental analysis of a sample.EDX examination was done on JEOL-JSM-6510LB.

High Resolution Transmission Electron Microscopy (HR-TEM)

HR-TEM is valuable technique used to study and identify the finest details of nanoparticles

Due to its high resolution (upto 200kV) lattice fringes of materials can be seen clearly.TEM (FEI Tecnai G2 F20, Netherlands) was used for study. For analysis of Se nanoparticles, 2µl of sample was loaded on C coated Cu grid and air dried for 30 min and visualized under 120 KV.

Gas Chromatography (CO_2 gas Analysis)

To estimate the amount of CO_2 evolved from the photocatalytic degradation process of 4-Chloroguaiacol, JOEL Analyzer (BGA) , AIMIL NUCON, equipped with Propak-Q column , automatic sampler and ECD detector, gas chromatograph was used to analyze the amount of CO_2 evolved from the photocatalytic degradation of 4-CG in the presence of Se@ZnO.

4. Results and Discussions

4.1 Section A: Biosynthesis and optio-structural analysis of Se NPs

Selected bacteria strain was cultured in TSA and active culture was taken for synthesis of Se^0. The strain was exposed with different concentration of sodium selenate in TSB staring from 10mM to 30 mM and incubated at 37˚C, on rotatory shaker at 120 rpm for 48 hr. The reduction of SeO_4^{2-} to Se^0 was detected by the formation of orange colored precipitates in the media shown in figure 1. Control reaction was carried out in same reaction conditions, by inoculating activated bacterial strain in TSB without sodium selenate. The color of the broth did not change, indicating no Se^0 production, thus the bacterial strain aerobically form Se NPs by reducing selenate ions (SeO_4^{2-}) into elemental Se^0. The active culture from plate (a) was taken and Streaked on 5 mM Se (sodium selenate) TSA plates (b and c).After the incubation period of 48 h, two distinct colonies of brick red (b) and orange (c) colour were observed indicating the growth of Se tolerant bacteria.

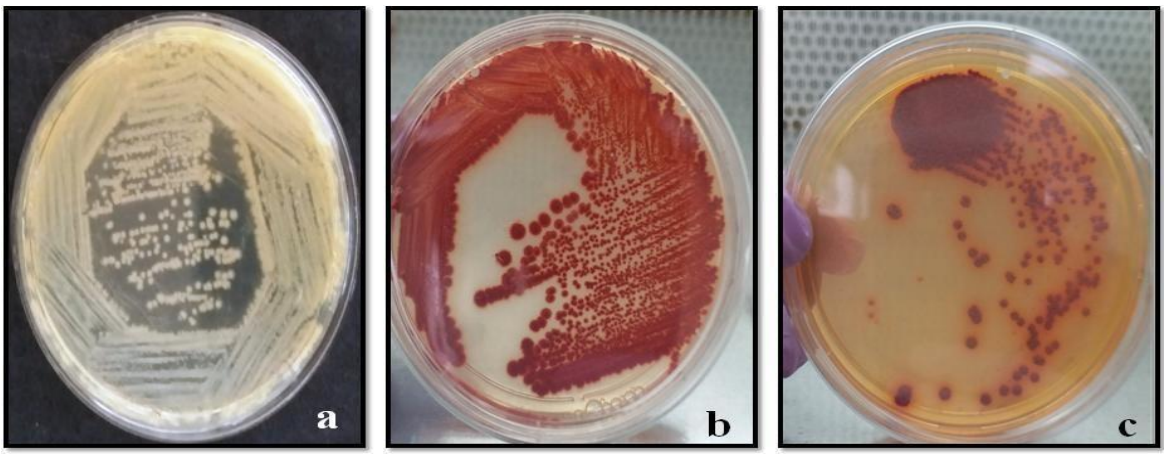

Fig. 1: (a-c) Isolated colonies of Se tolerant bacteria on Trypton Soya Agar (TSA) (a) Control Plate without Se (Na_2SeO_3), (b) Red colored colonies on 5mM Se (as Na_2SeO_3) TSA plate indicating Intracellular production of Se, (c) Orange colored colonies on 5mMSe (as Na_2SeO_3) TSA plates showing extracellular production of Se.

The strain was exposed with different concentration of sodium selenate in TSB staring from 10mM to 30 mM and incubated at 37˚C, on rotatory shaker at 120 rpm for 48 hr. The reduction of SeO_4^{2-} to Se^0 was detected by the formation of orange colored precipitates in the media shown in figure 1. Control reaction was carried out in same reaction conditions, by inoculating activated bacterial strain in TSB without sodium selenate. The color of the broth did not change, indicating no Se^0 production, thus the bacterial strain aerobically form Se NPs by reducing selenate ions (SeO_4^{2-}) into elemental Se^0. The active culture from plate (a) was taken and Streaked on 5 mM Se (sodium selenate) TSA plates (b and c).After the incubation period of 48 h, two distinct colonies of brick red (b) and orange (c) colour were observed indicating the growth of Se tolerant bacteria.

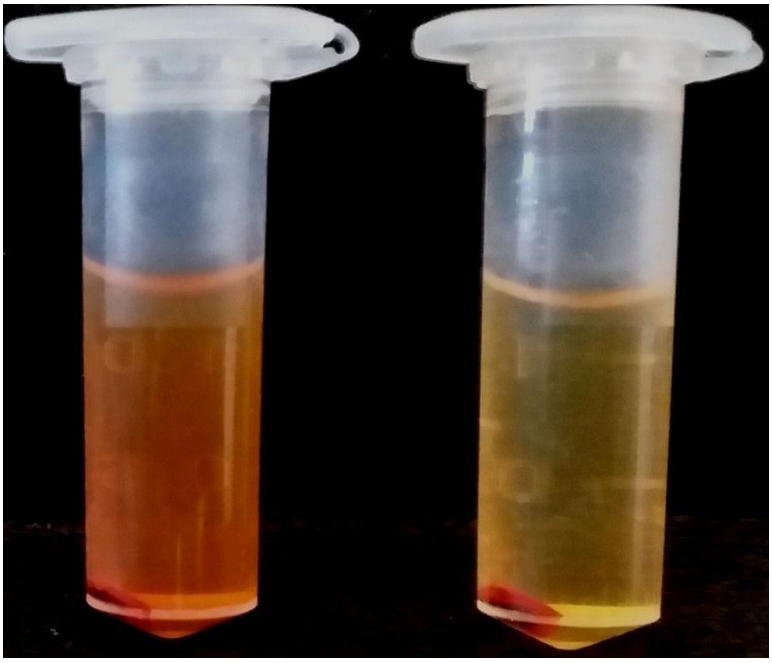

Fig.2: (a) Extracellular (orange colour) Se and (b) Intracellular Se nanoparticles

The orange color obtained in figure 2 obtained by centrifugation (5000 rpm, 5min) of bacterial cells in TSB confirms the extracellular production of Suspended Se NPs and yellow color media obtained after centrifugation (5000 rpm, 5min) of bacterial cells in TSB confirms the extracellular production of Se NPs as bacterial pellet was settled down along with the nanoparticles present inside the bacterial cell.

Fig.3: Gram staining representing the rod shaped gram negative, Bacterial strain of *Bacillus sp.*

bacteria was identified by differential Gram staining technique. Figure 3 shows the rod shaped pink color Gram negative bacteria

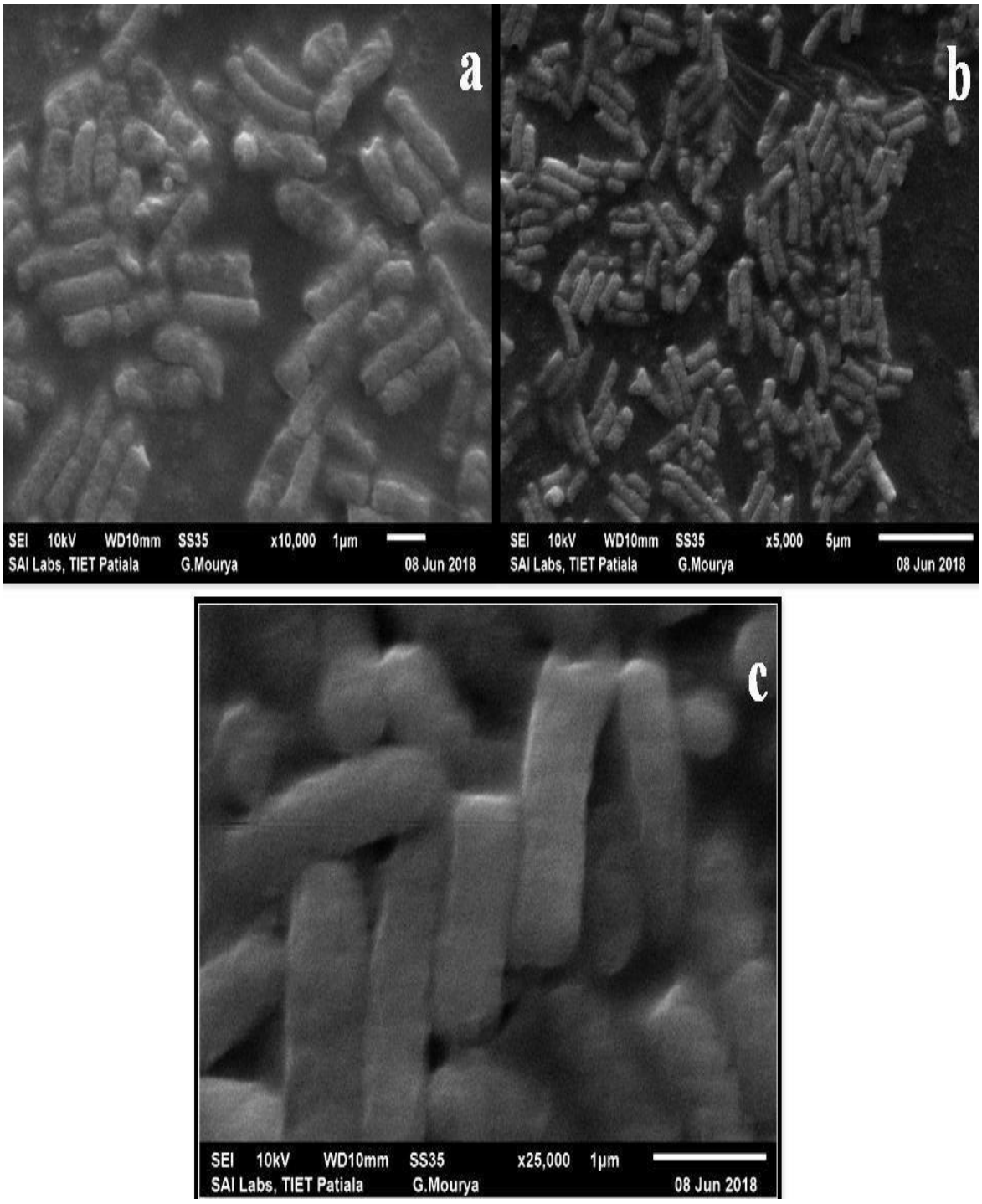

Fig.4: (a-c) SEM Morphograph of Se tolerant Bacteria

The UV-Vis spectrometric analysis, (figure 5), was done by scanning the Se NPs suspension in the range of 200-1100 nm. The characteristic absorbance peak was observed at 658 nm which corresponds to particle size of 160 ± 10.2 nm shown in the figure 6.

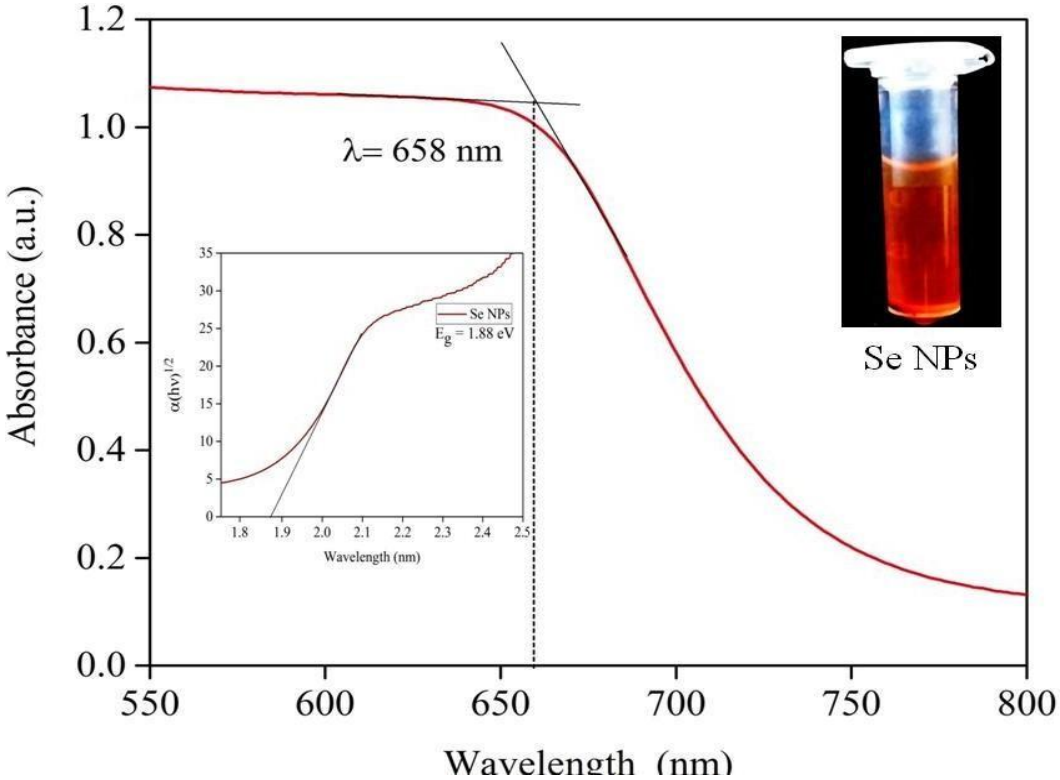

Fig. 5: UV-DRS spectrum of Se nanoparticles with inset of Tauc plot.

The band gap (Eg) of Se NPs was calculated using the equation: Eg (eV) = 1240/λ

Eg (eV) = 1240/658 = 1.88 eV

Eg- Band gap (in electron volt)

λ - Wavelength (nm) at absorbance maxima.

Further, Optical band gap Se NPs was calculated by using Tauc's relation $(\alpha h\upsilon)^{1/n} = A (h\upsilon - E_g) = 1.88$ eV

Where, α - Absorption coefficient of material

h- Planck constant

υ- Frequency of light

n- Exponent characteristic of type of electrons Transition process (n=1/2 for direct allowed transition & n= 2 for indirect allowed transition process

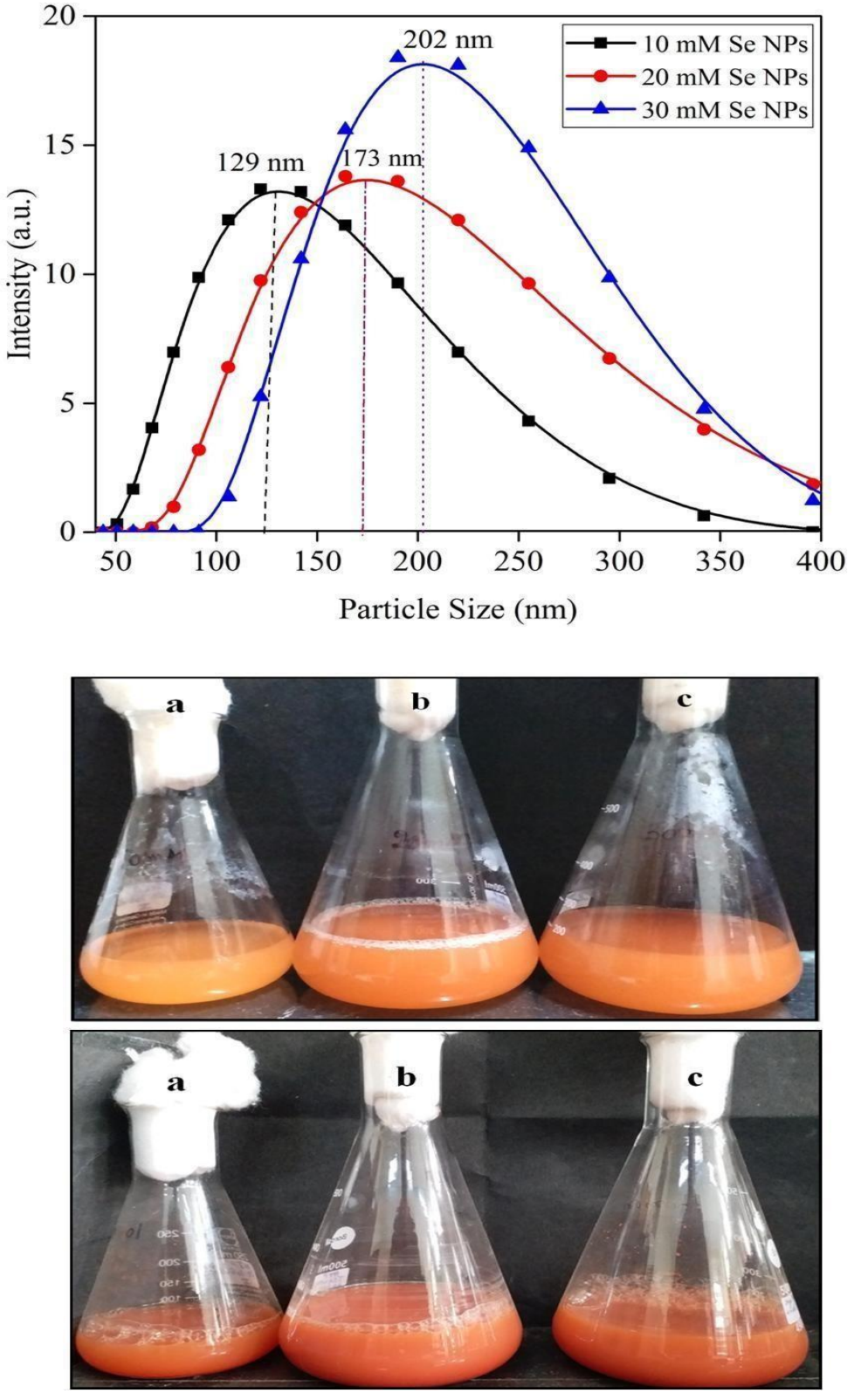

Fig.6: Average hydrodynamic size of Se nanoparticles biosynthesized at different concentration of Se. (a-c) 12 hr production flasks of bacteria showing growth in TSB at different concentration of Se (as Na_2SeO_3), (a) 10 mM, (b) 20mM, (c) 30mM and (a-c) 24 h production flasks of bacteria showing growth in TSB at different concentration .

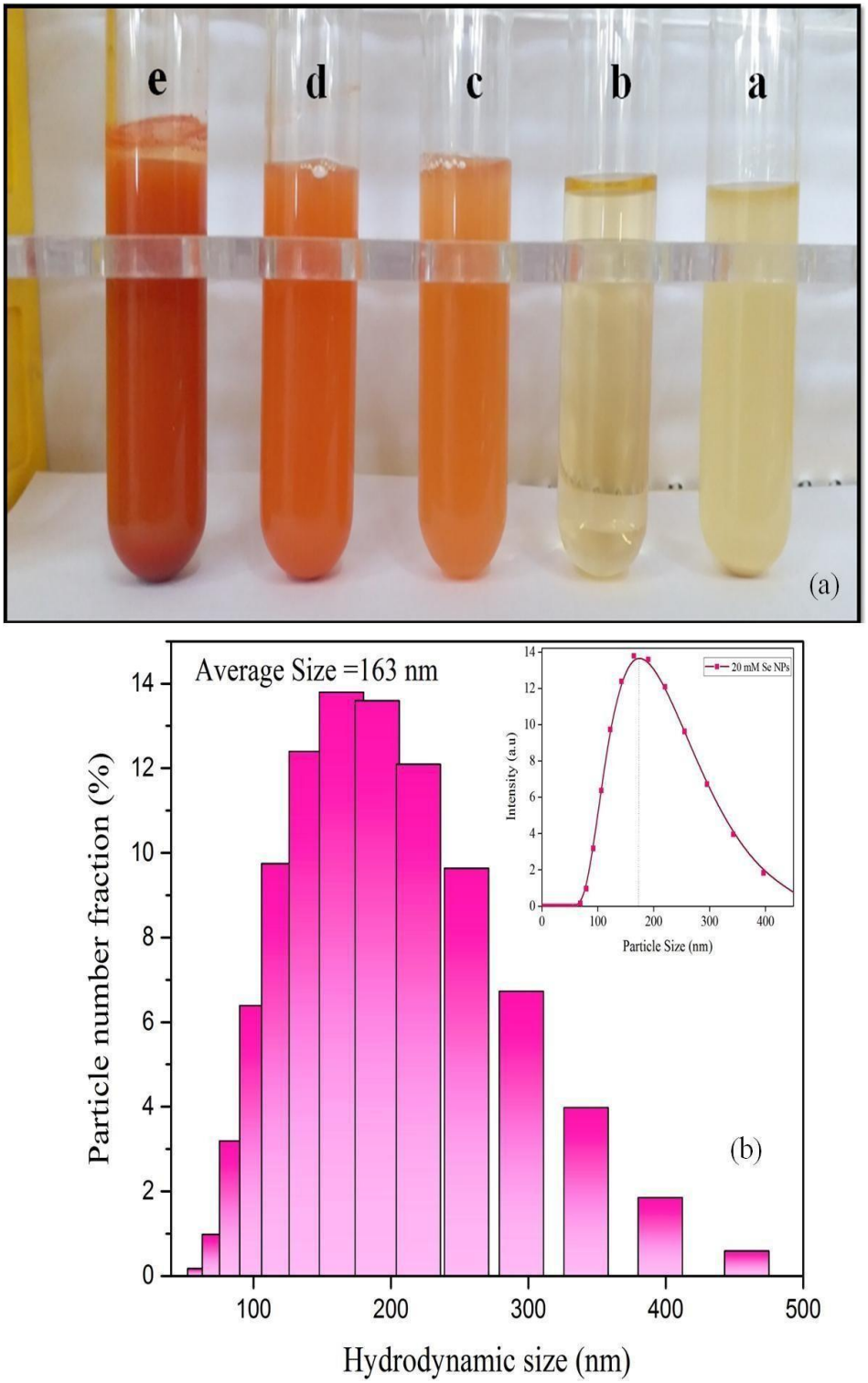

Fig.7: (a) Time dependant growth of Se tolerant bacteria in 20 mM TSB and (b) Average hydrodynamic of Se nanoparticles after 48h.

A time dependent growth (0h to 48h) showed (figure 7 a) the change in intensity of color from very light yellow to intense orange color in sample incubated at 37ºC for 48 h. The change in characteristic color of TSB was due to excitation of surface plasmon vibrations of the α-Se formation. In control reaction broth (a), no change in color of the sample was observed, which confirms that the formation of biogenic Se NPs was only due to the bacteria and its capped protein. Due to high temperature and pressure of autoclave the bacterial cells were killed and its proteins were degraded. The average size of the prepared Se NPs after 48h was observed as 163 nm shown in figure 7 (b).

The surface morphology of the bacterial cells associated with Se NPs is shown in figure 8.

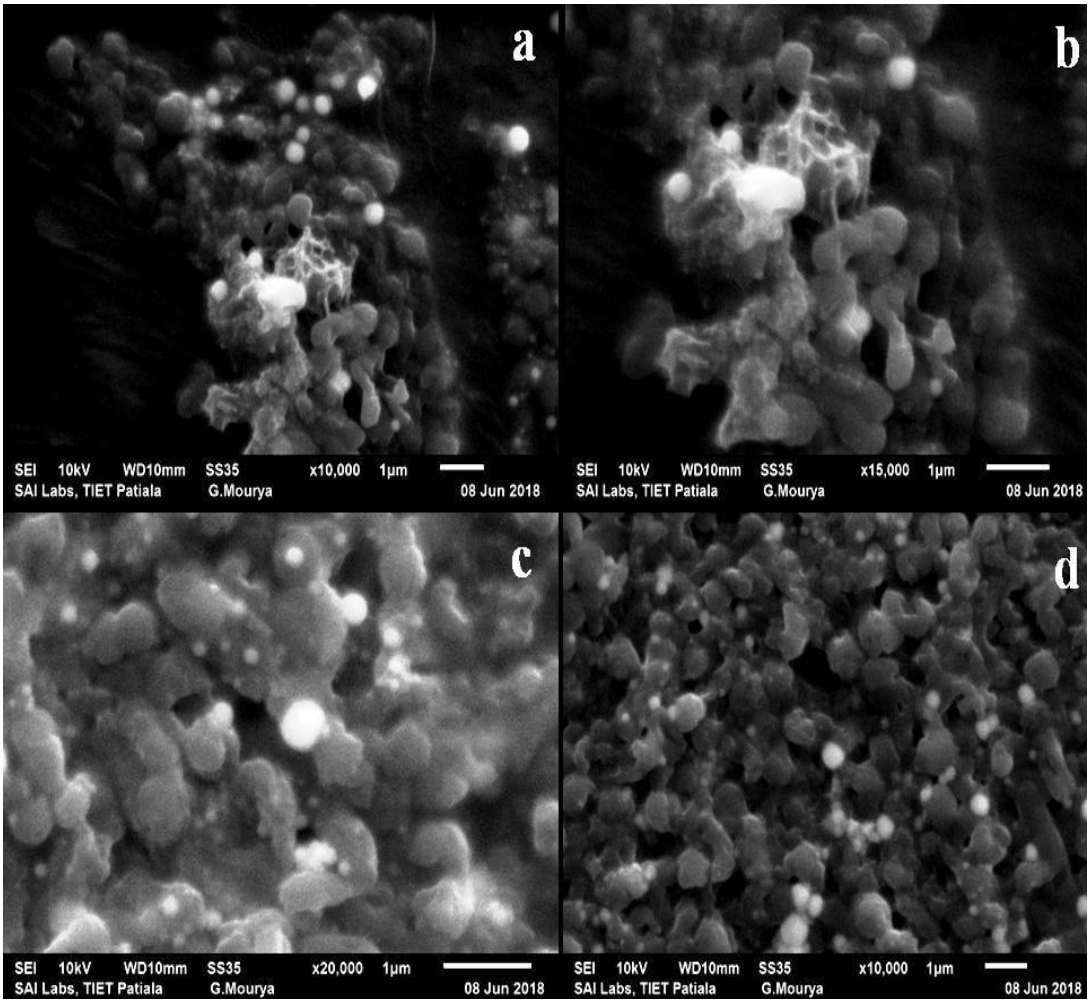

Fig.8: SEM images of 48h incubated bacterial cells associated with Se nanoparticles.

Spherical shaped Se NPs were observed with uniform distribution in figure 9. The NPs were in size range of 130- 160 nm. Highly monodisperse nature of the particles was seen. The corresponding EDX spectrum of the prepared Se NPs (figure 10) confirms the sole presence of Se in the NP solution and STEM was shown in figure 11.

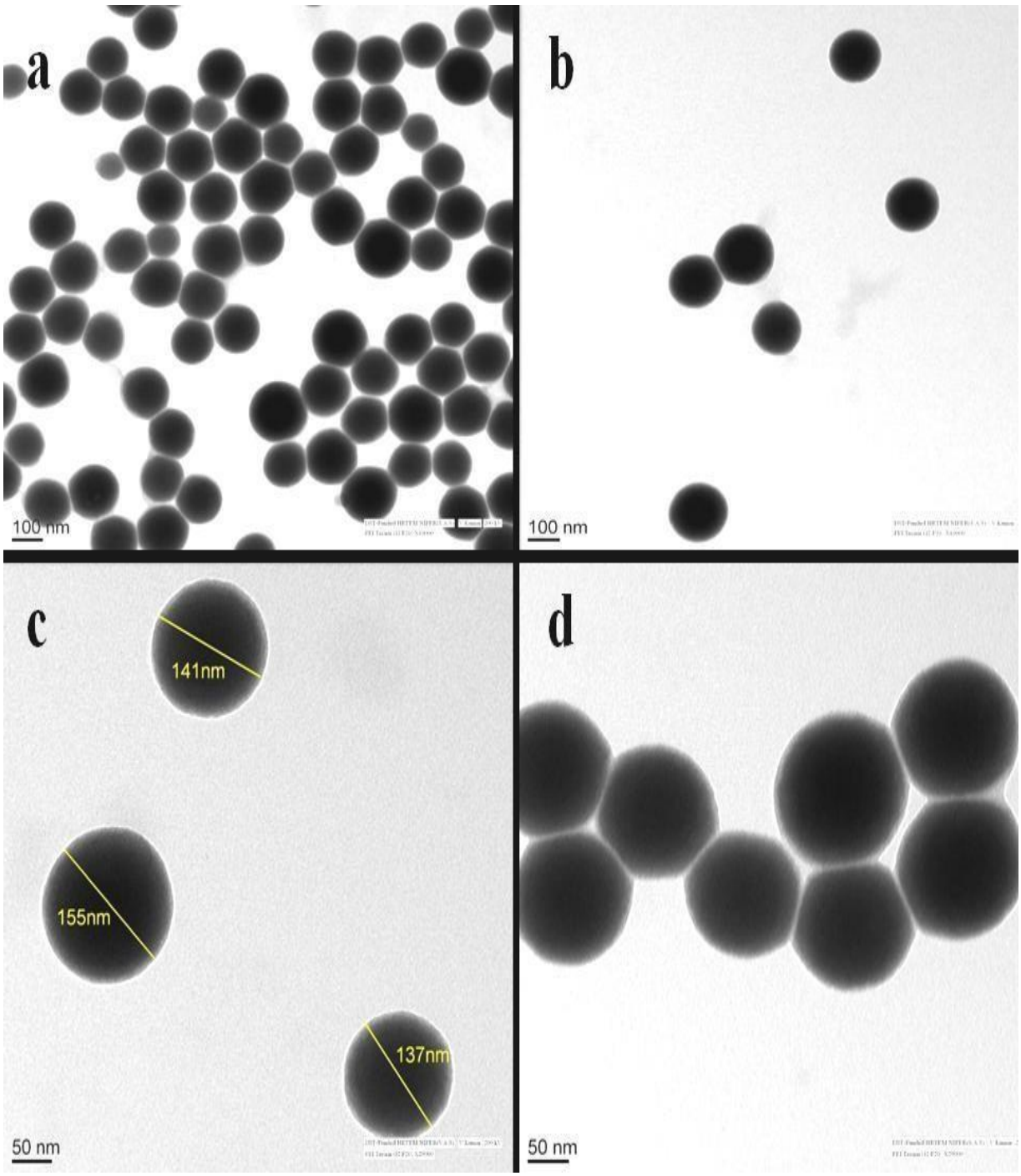

Fig.9: TEM images of Se nanoparticles.

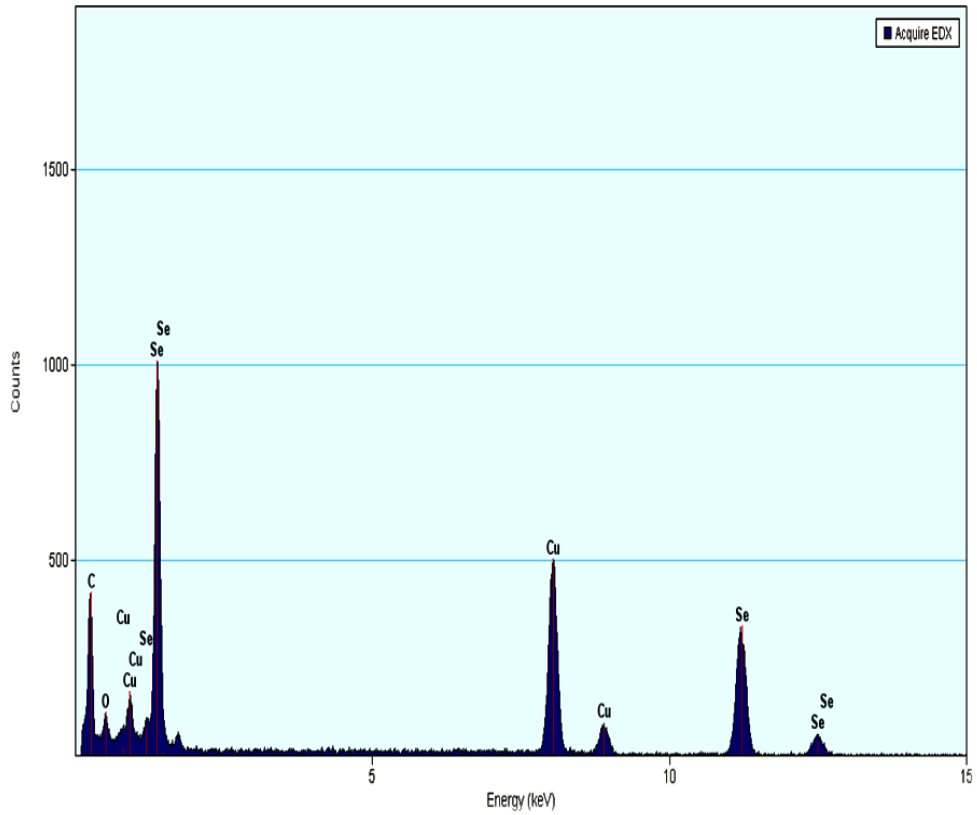

Fig.10: EDX profile of Se nanoparticles.

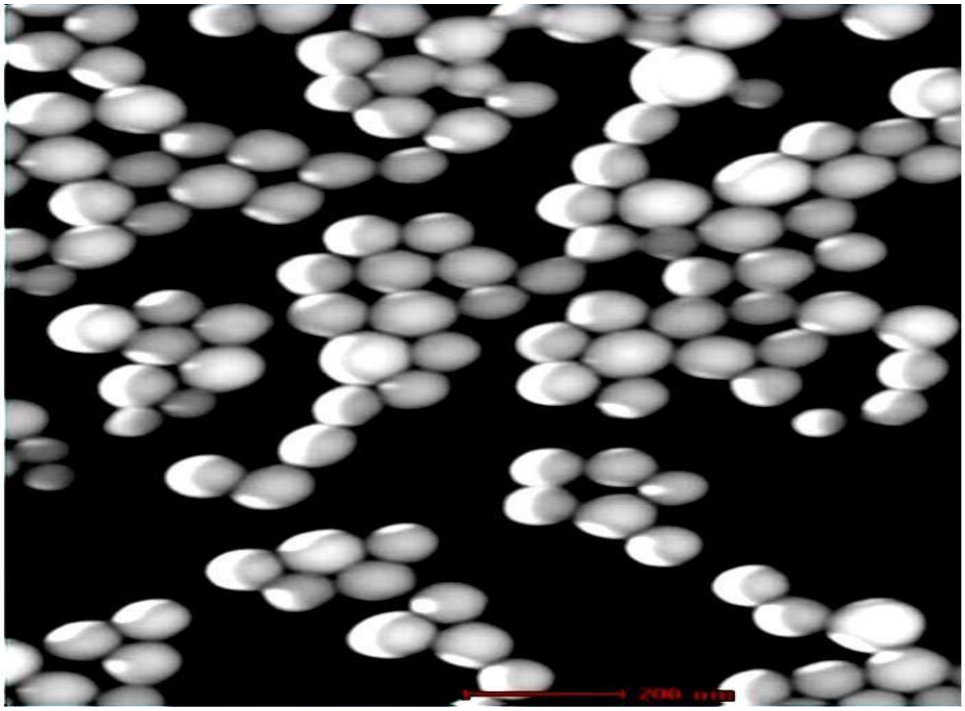

Fig. 11: STEM Image of Se nanoparticles

Section B: Optical and Structural Analysis of Se@ZnO nanocomposites

Pure ZnO is seen to show λ_{max} at 381 nm as observed from DRS spectrum in figure 12(a).

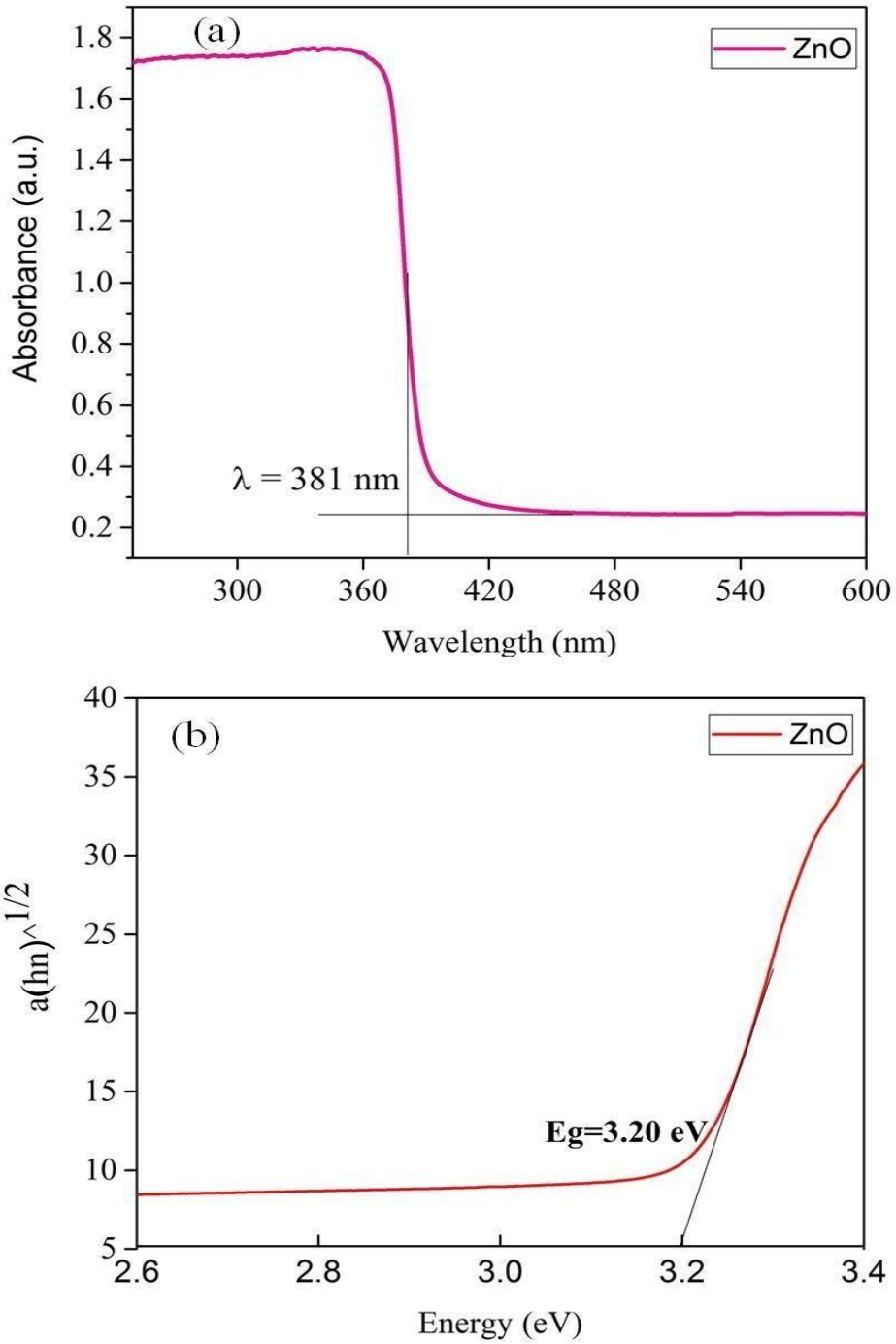

Fig. 12: (a) DRS spectrum and (b) Tauc plot of pure ZnO.

The band gap of pure ZnO NPs calculated using Tauc plot was obtained to be 3.20 eV as shown in figure 12(b).

Similarly, the DRS spectra of different (0.5-2) wt% Se doped ZnO nanocomposites was observed as shown in figure 13. It was seen that compared to pure ZnO, the Se doped ZnO nanocomposites showed a red shift towards higher wavelength at λ_{max} 658 nm which indicated the presence of Se which acts as a biophotonic agent.

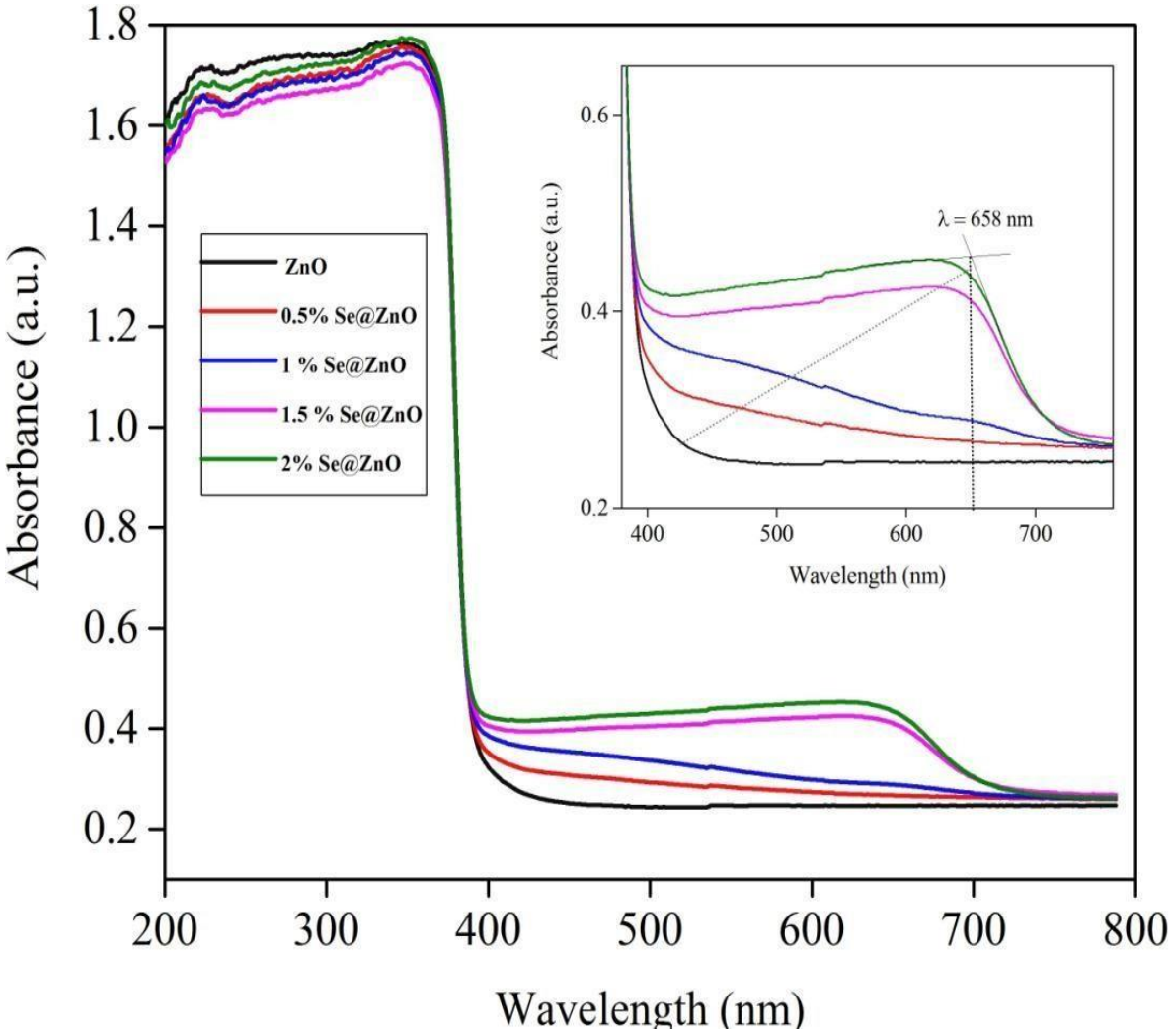

Fig. 13: DRS spectra of different wt% (0.5-2) Se doped ZnO nanocomposites in visible region and inset shows the magnified view of the spectra.

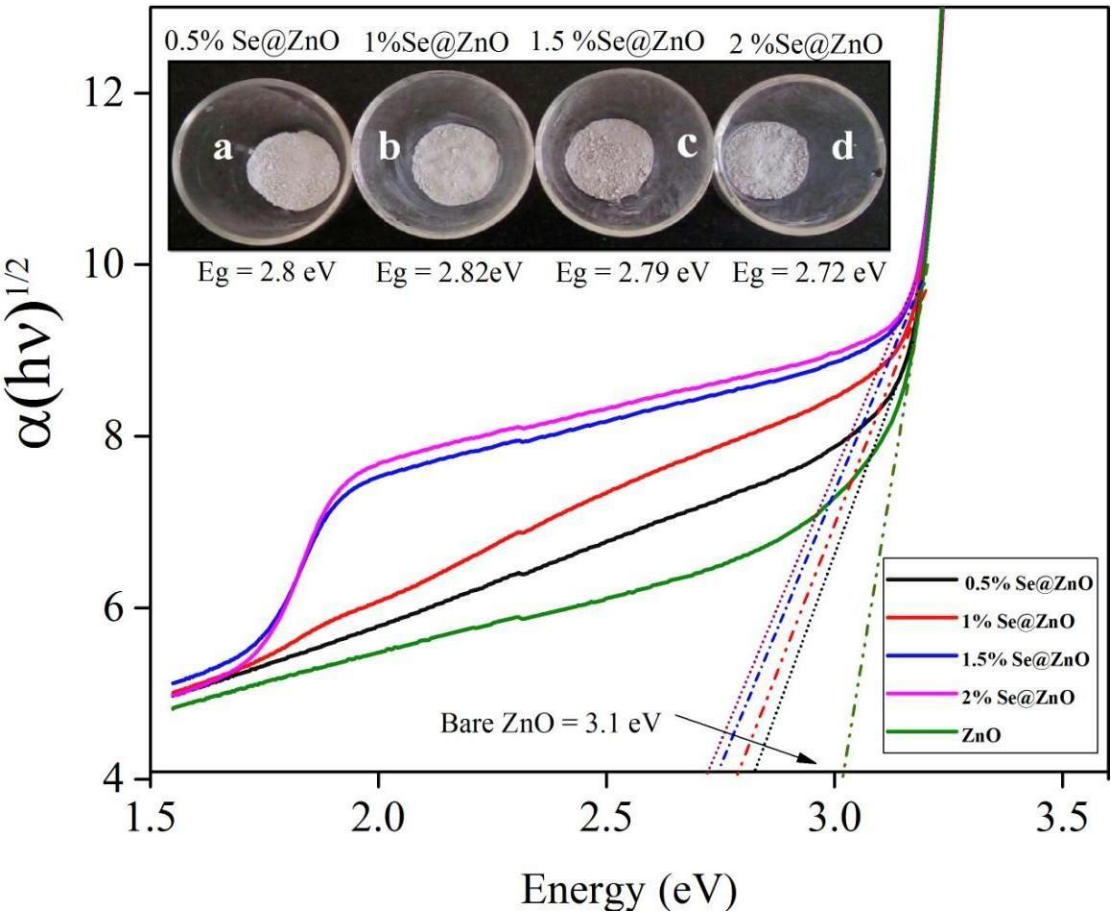

Fig. 14: Tauc plot of Se@ZnO nanocomposite with increasing (0.5-2) wt% of Se doping.

A decrease in the E_g (2.8 eV) was observed for Se@ZnO nanocomposite compared to pure ZnO shown in figure 14. It was observed that as the amount of Se doping over ZnO was increased from 0.5 to 2 wt% the E_g further decreased to 2.72 eV.

The crystalline structure of synthesized photocatalyst was confirmed using X-ray diffractrometer using Cu Kα radiation source (α = 1.5406 Å), 2θ ranging from 20° to 80°, operated at an accelerating voltage of 45 kV and 40 mA applied current and is shown in figure 15.. The peaks appearing at 2θ, 30.30°, 35.21° (101), 50° (102), 60°(110) 63.18° (103) and75.9° (202) corresponds to the hexagonal wurtzite structure of ZnO (JCPDS N0. 80:0075) and (JCPDS N0.36-1451). The strong diffraction peak appearing at 30.30° (101) corresponds to the hexagonal selenium phase [26]. Hence, XRD result shows the successful biological synthesis of Se@ ZnO nanocomposite.

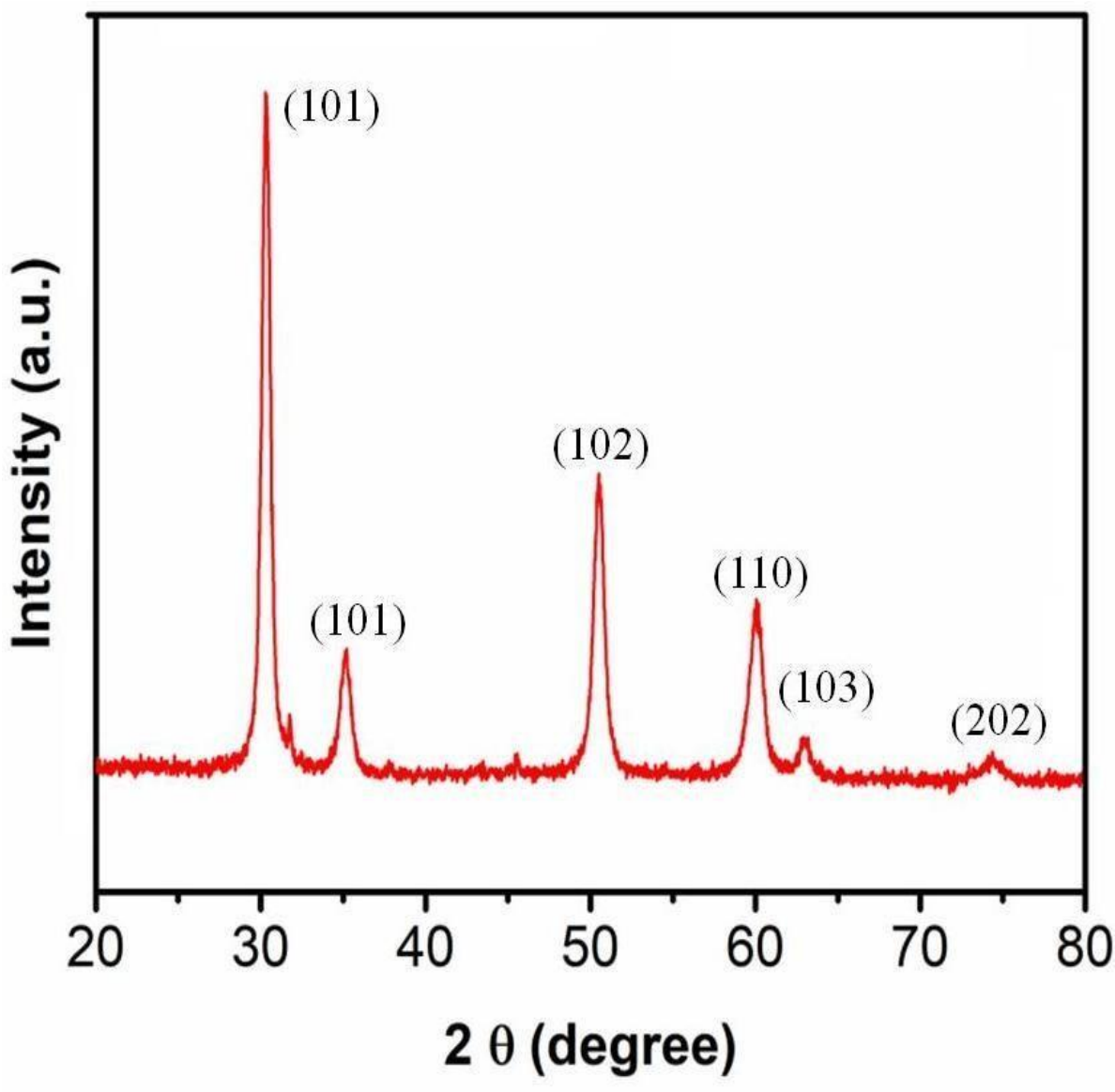

Fig. 15: XRD of 0.5 wt% Se doped ZnO nanocomposite.

SEM images of pure ZnO and 0.5wt% Se@ZnO nanocomposite are shown in figure 16. It was observed that the hexagonal wurtzite structure of ZnO was not affected when it was doped with 0.5 wt% of Se or 1 wt% of Se (figure 17). However, when the wt% of Se doping was increased a distortion in the structure of ZnO was seen in figure 18.

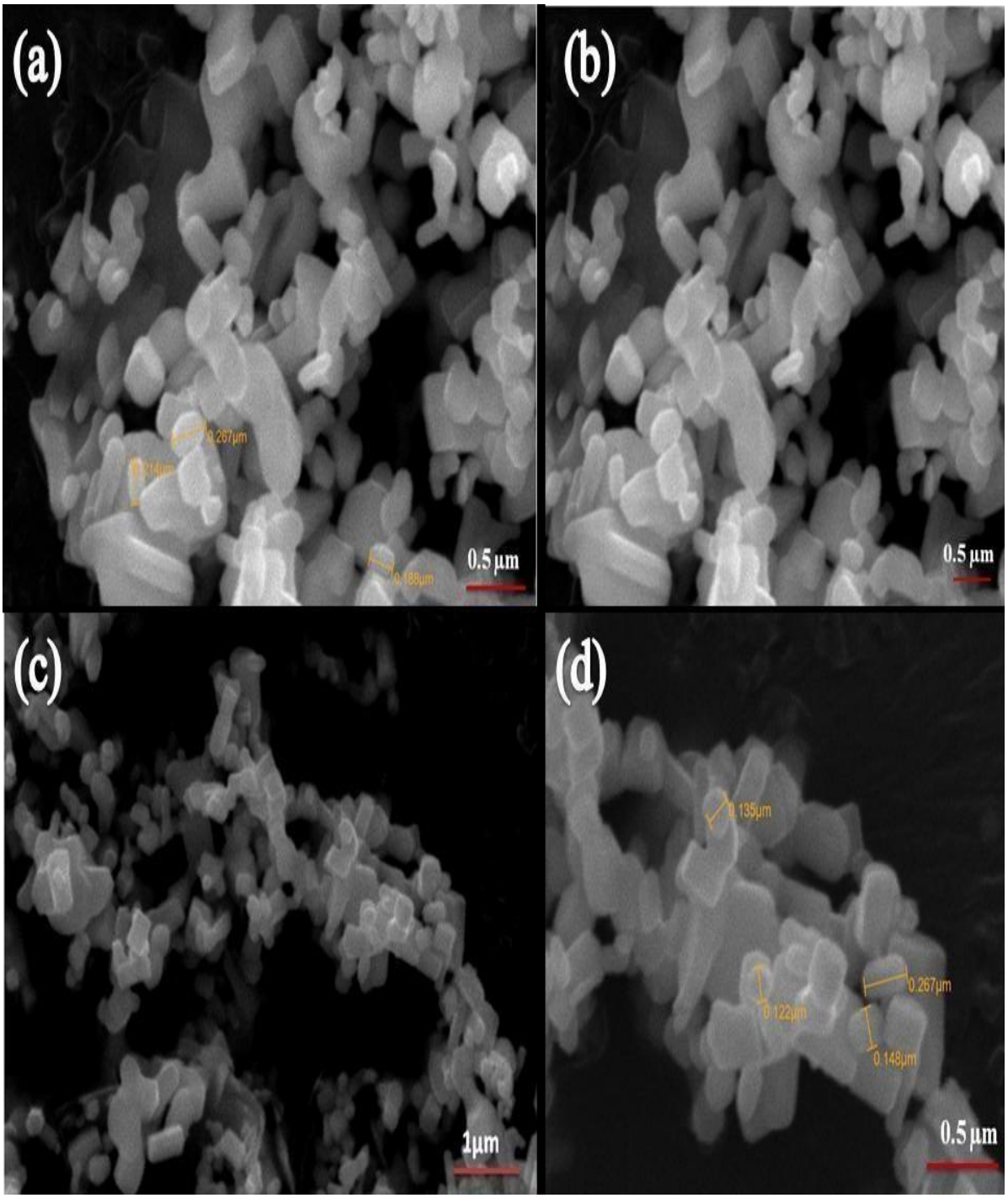

Fig 16: SEM of (a-b) pure ZnO and (c-d) 0.5wt% Se@ZnO nanocomposite.

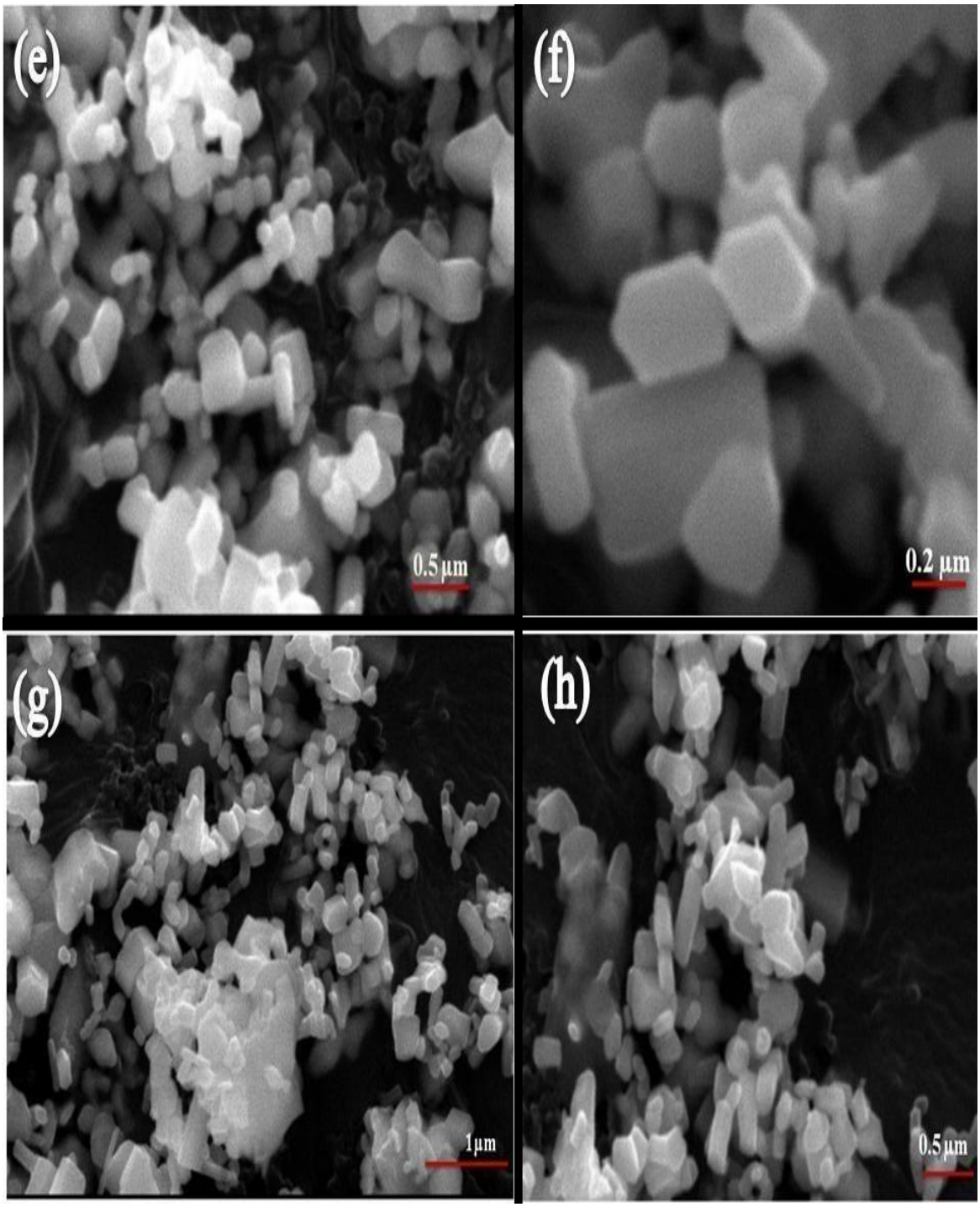

Fig 17: SEM of (e-f) 1 wt% and (g-h) 1.5wt% Se@ZnO nanocomposite.

The elemental analysis and increasing wt% (0.5-2) of Se doping over ZnO was further confirmed by EDX spectra shown in figure 19.

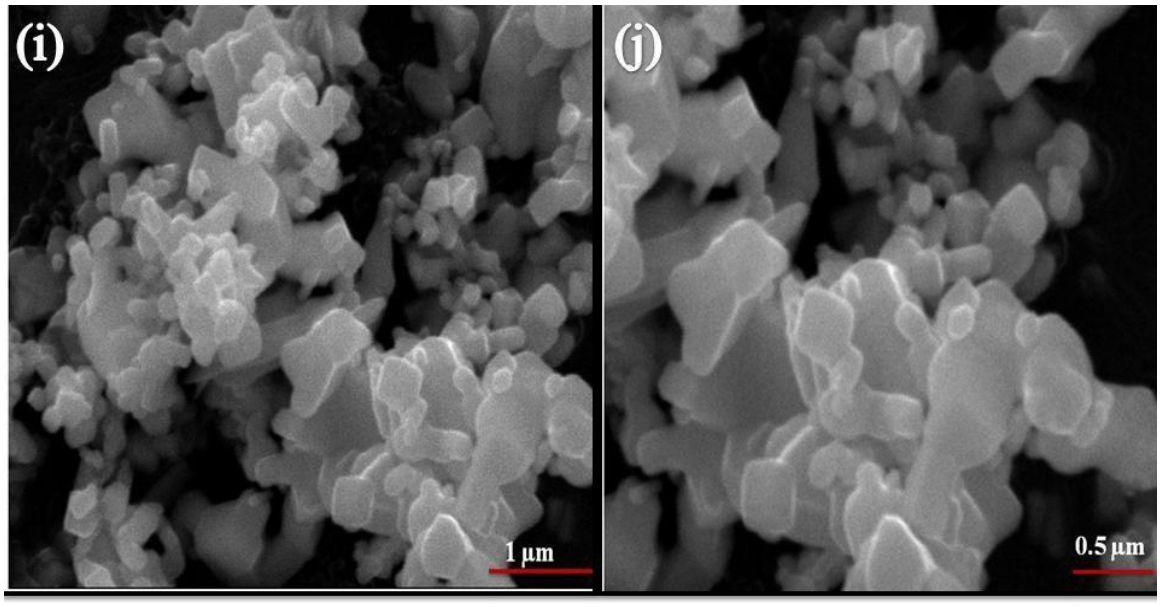

Fig 18: SEM of 2wt% Se@ZnO nanocomposite.

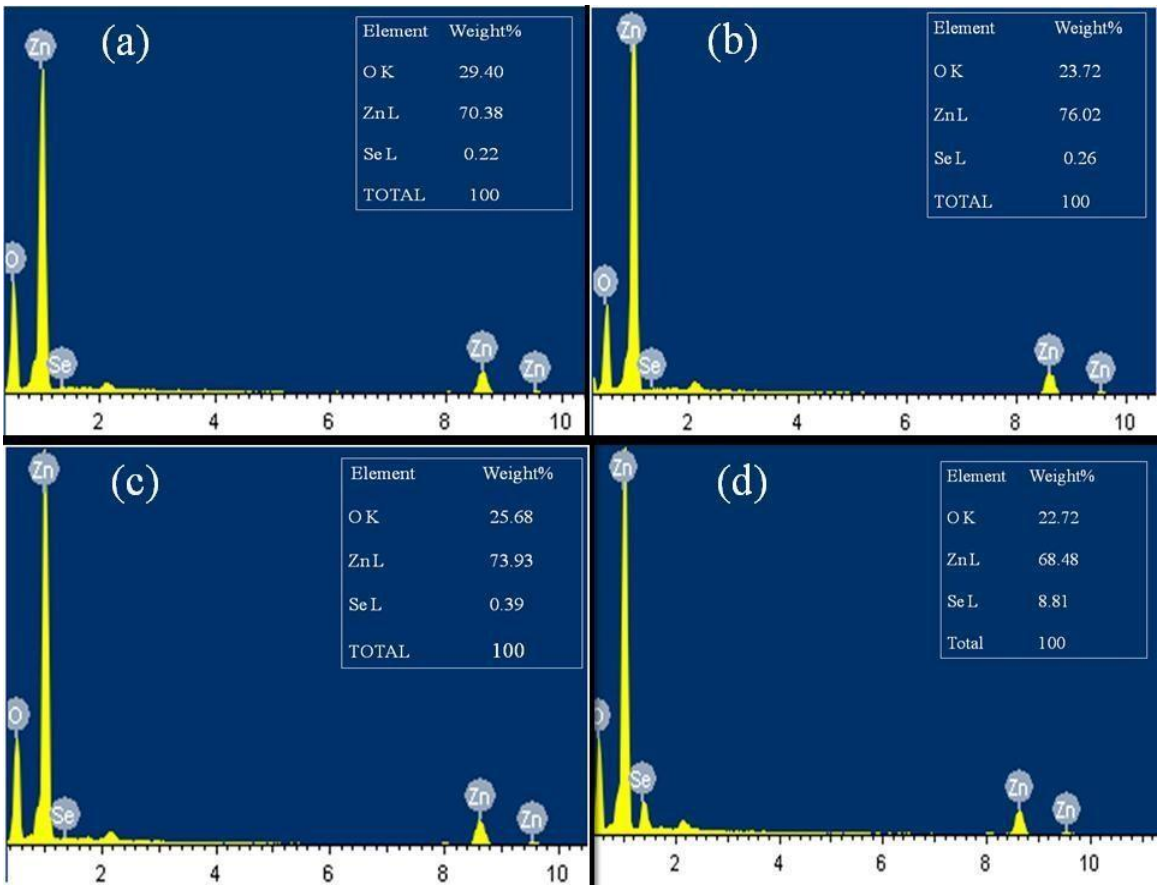

Fig. 19: EDX of (a) 0.5wt%, (b) 1 wt%, (c)1.5 wt% and (d) 2 wt% Se@ZnO.

Section A: Dark adsorption of 4-Chloro guaiacol (4-CG)

Calibration graph of 4-Chloro guaiacol pollutant

To study the dark adsorption and photocatalytic degradation of 4-CG first we make calibration graph of 4-CG. Absorbance of each 4-CG solution was measured with double beam UV visible spectrophotometer and calibration graph between absorbance vs. concentration was plotted.

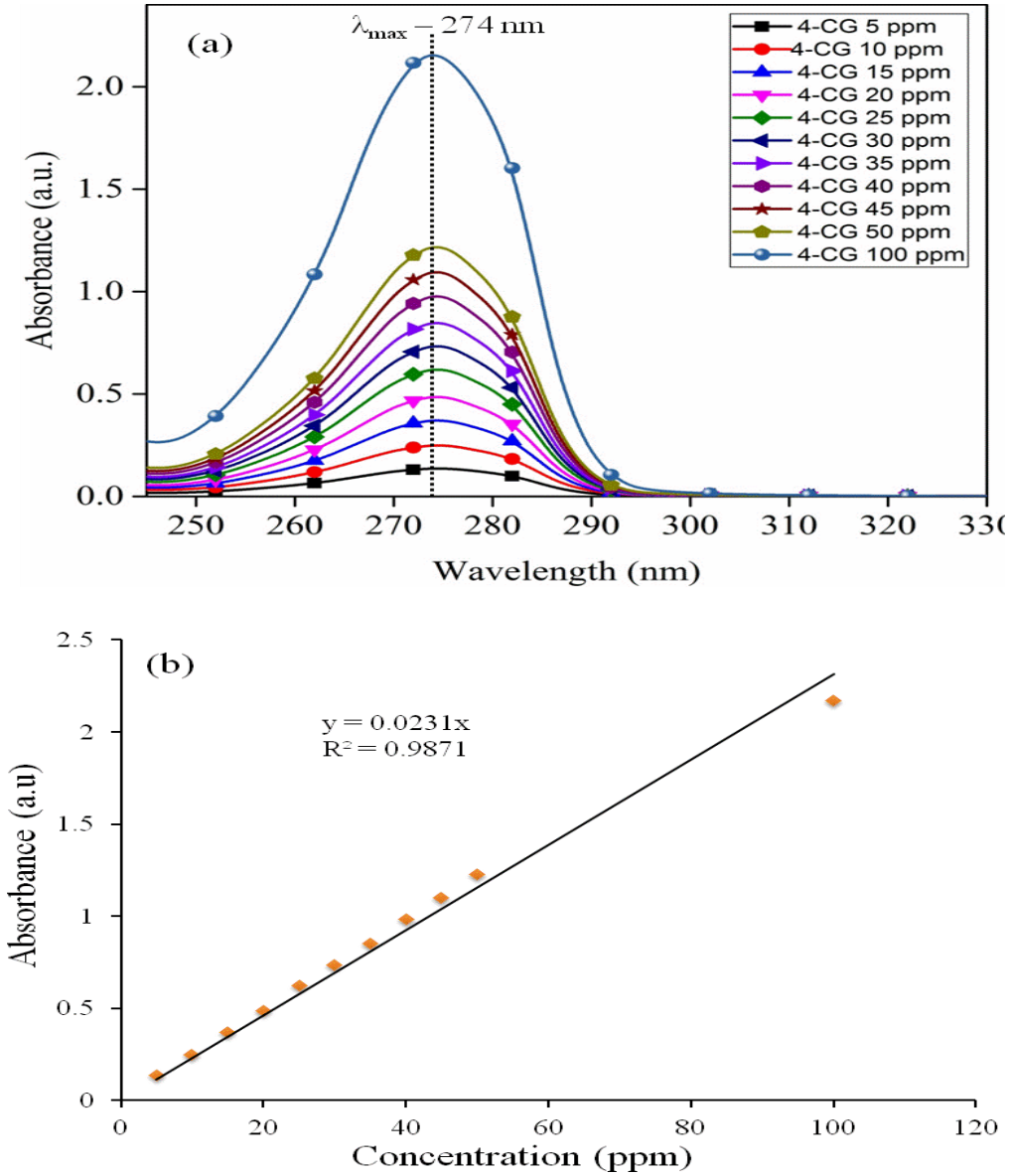

Fig. 20: (a) Absorbance spectra and (b) Calibration graph (absorbance vs. concentration) of 4-Chloro guaiacol pollutant.

Figure 21 shows the dark adsorption of 4-CG (20 ppm), the value of absorbance observed indicated that it follows beer lamberts law.

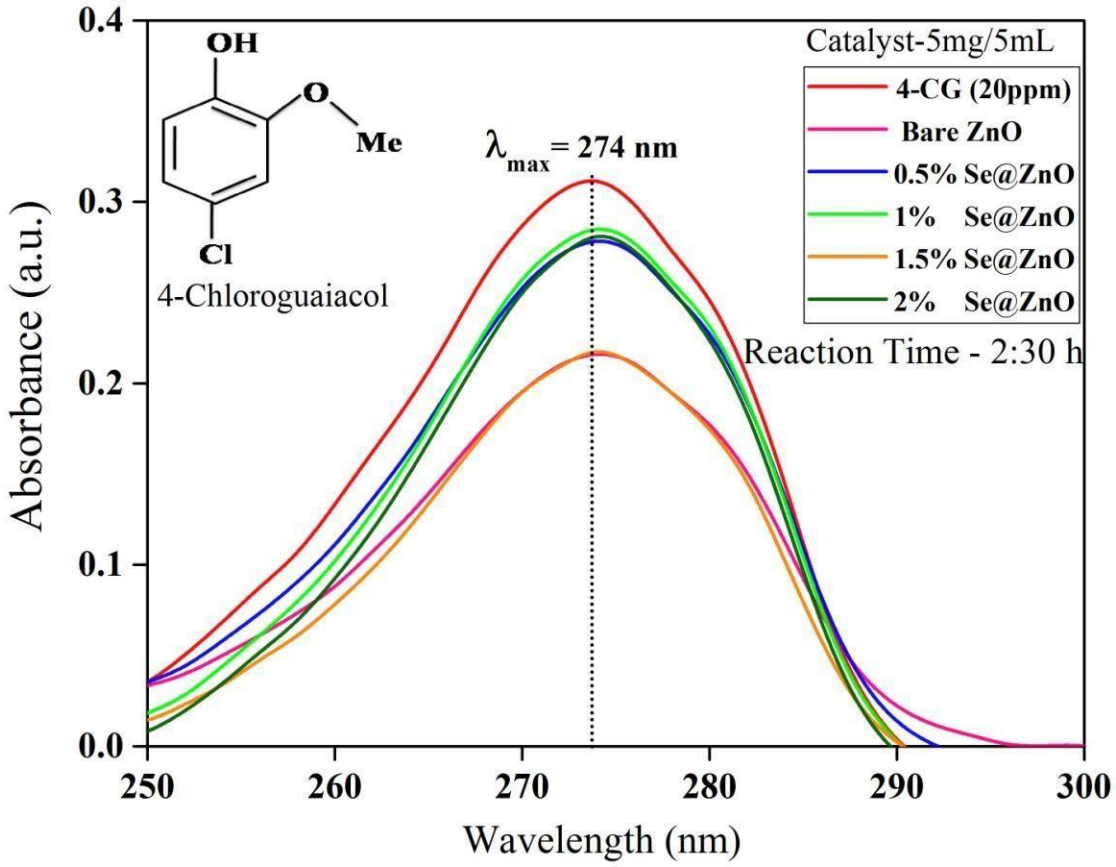

Fig. 21: Effect of different concentration of 4-CG pollutant on adsorption of Se@ZnO.

Section B: Photocatalytic activity of Se@ZnO for photo degradation of 4-Chloro guaiacol

The absorption spectrum of 4-CG (20 ppm) photo degradation by Se@ZnO was obtained after 15 min sunlight irradiation shown in figure 22. It was observed that 0.5wt and 1.5 wt% Se@ZnO showed the best catalytic efficiency, as a decrease in the absorbance value from 0.289-0.02 a.u. 93% of photo degradation efficiency was obtained for 0.5 wt% Se@ZnO after 105 minutes of sunlight irradiation shown in figure 23.

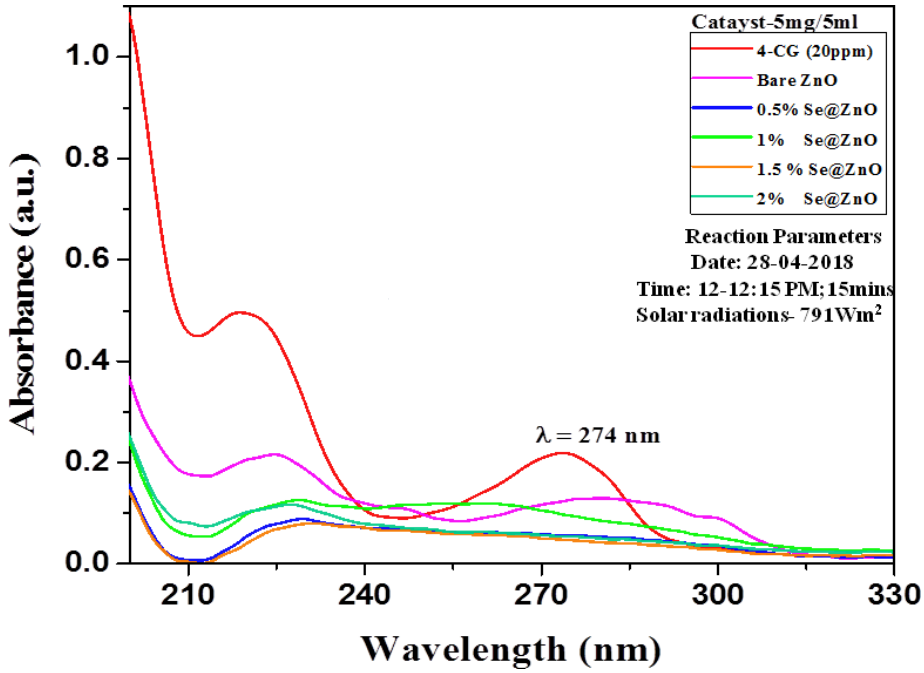

Fig. 22: Comparative absorption spectra of 4-CG (20 ppm) due to its photo degradation by different (0.5-2) wt% Se over ZnO sample obtained after 15 min under sunlight irradiation.

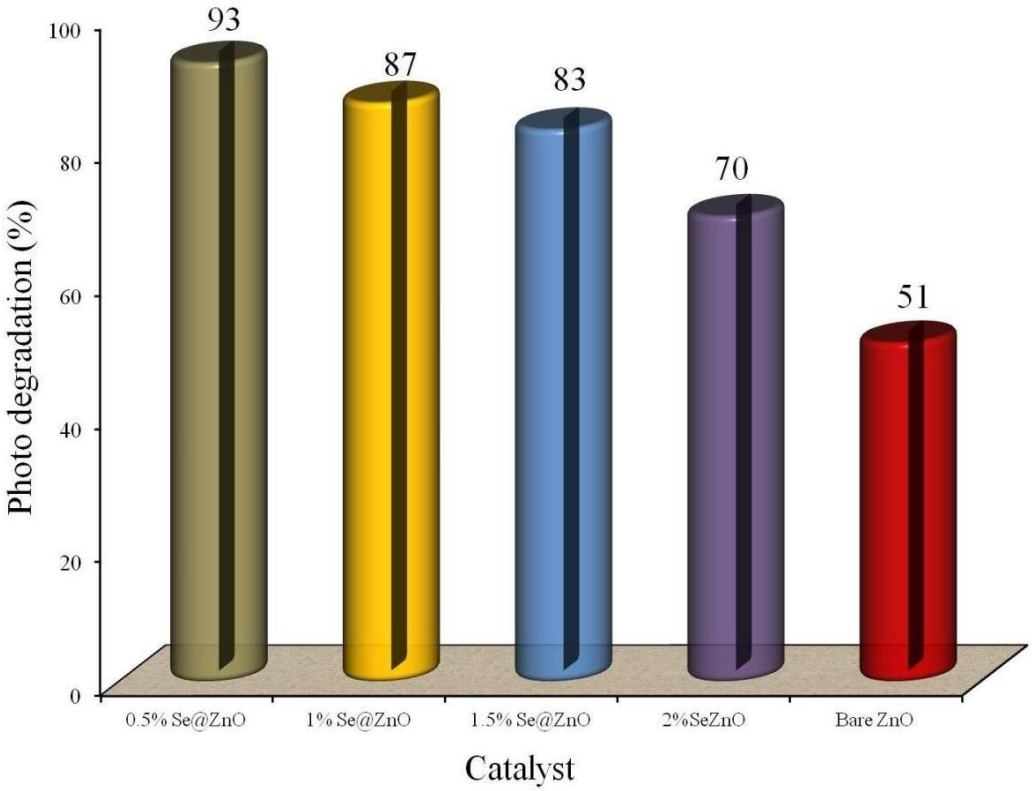

Fig. 23: Comparative photodegration efficiency of 4- Chloro guaiacol (20 ppm) by (0.5-2) wt% Se@ZnO photocatalyst under 15 min sunlight irradiation.

Similarly, the absorption spectrum of 4-CG (50 ppm) photo degradation by Se@ZnO was obtained after 15 min sunlight irradiation shown in figure 24. A shift in the degradation pattern was observed which can be attributed to intermediate formation and simultaneous degradation of 4-CG takes place as the absorbance value decreases from 0.93 to 0.065 a.u.

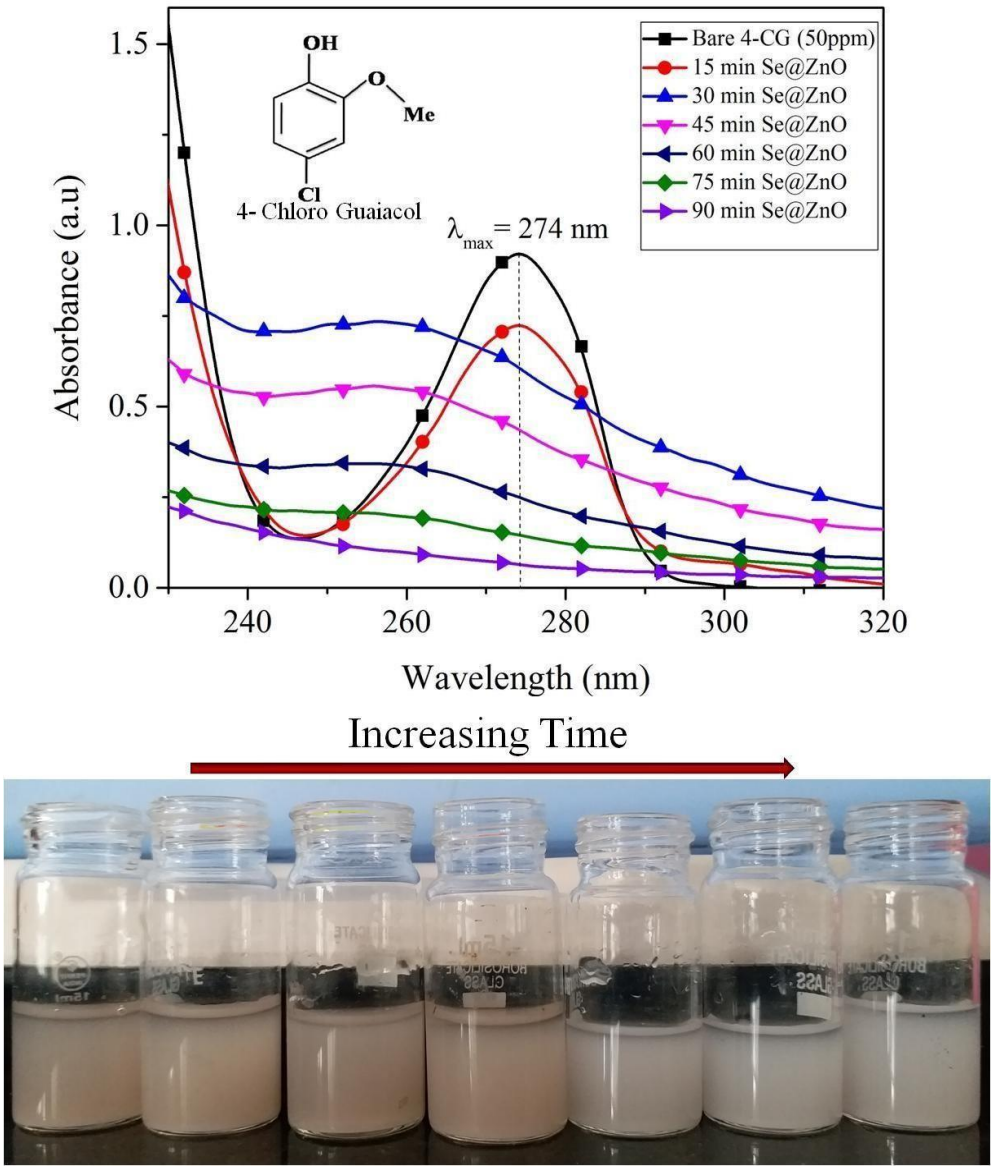

Fig. 24: Comparative absorption spectra of 4-CG (50 ppm) due to its photo degradation by different (0.5-2) wt% Se over ZnO sample obtained after 15 min under sunlight irradiation and change in colour intensity after increasing time interval from 15-90 min.

This higher catalytic efficiency exhibited by the photocatalyst can be attributed to the combined co-catalytic effects of Se which helps in the increase in interfacial contact area, leading to increased transfer of charge and decreased recombination rate of charge carriers because of synergistic effect of Se.

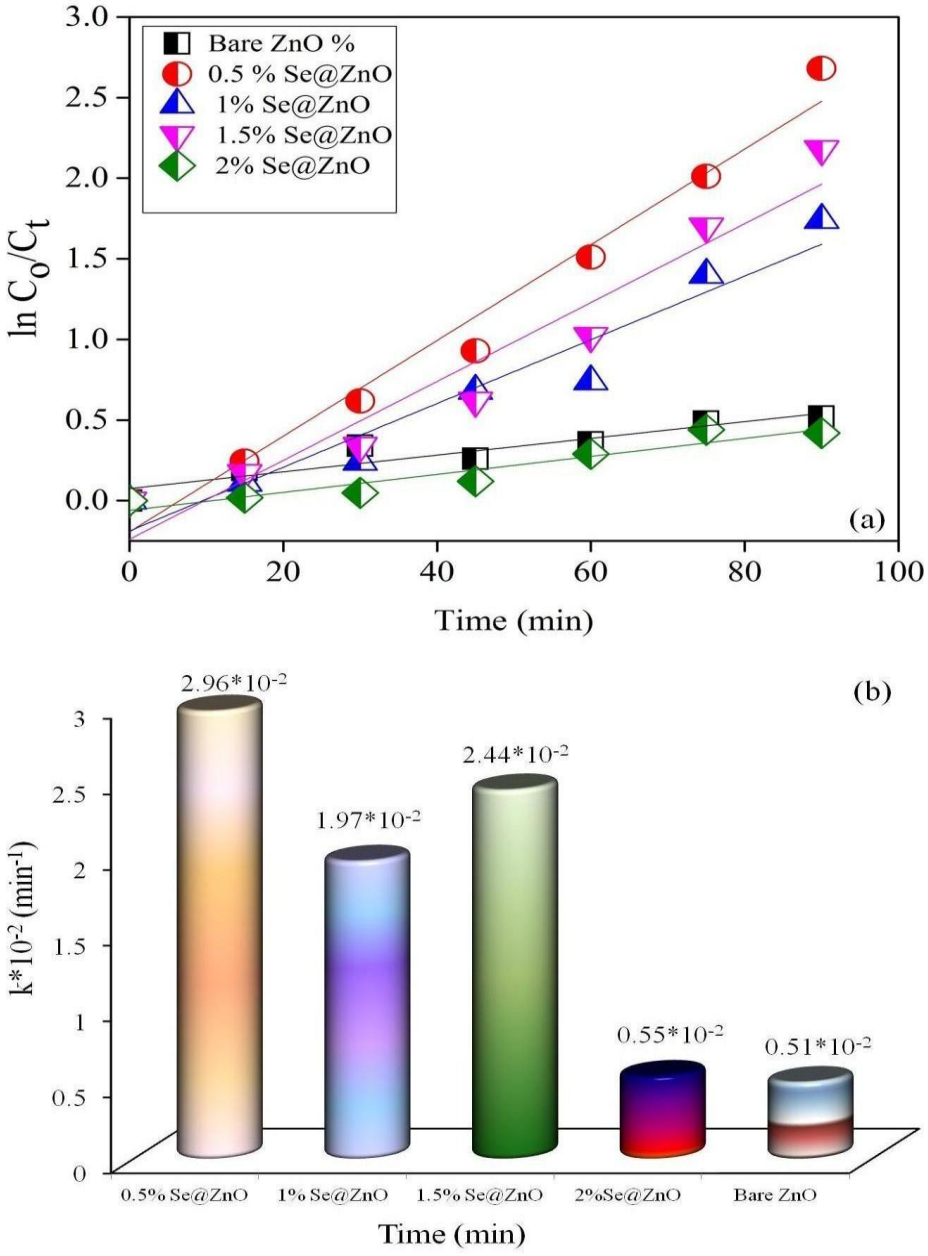

Fig. 25: (a) Time course of 4-CG (50 ppm) photo degradation by (1-2) wt% Se@ZnO obtained with sunlight irradiation for 90 minutes and (b) Comparative rate constant of different Se@ZnO catalyst.

Figure 25 shows the log C_0/C_t Vs time (min) graph where C_0 is the initial concentration and C_t is the concentration at different time intervals of 4-CG photo degraded by 0.5-2 wt % Se over ZnO for 90 min. Pseudo first order rate kinetics was observed according to the equation:

$2.303 \log C_0/C_t = kt$

Where, k is the rate constant for pseudo first order rate kinetics. It was seen that in the absence of the catalyst, zero or negligible photo degradation indicating the need of photocatalyst to initiate the photolysis process. The k values for (0.5-2) wt % Se@ZnO catalyst photo degraded 4-CG for 15-90 min was $2.96*10^{-2}$ min^{-1} to $0.55*10^{-2}$ respectively and the regression coefficient (R^2) value of 0.972 is in good concurrence. 93% of photo degradation efficiency was obtained for 0.5 wt% Se@ZnO after sunlight irradiation shown in figure 26.

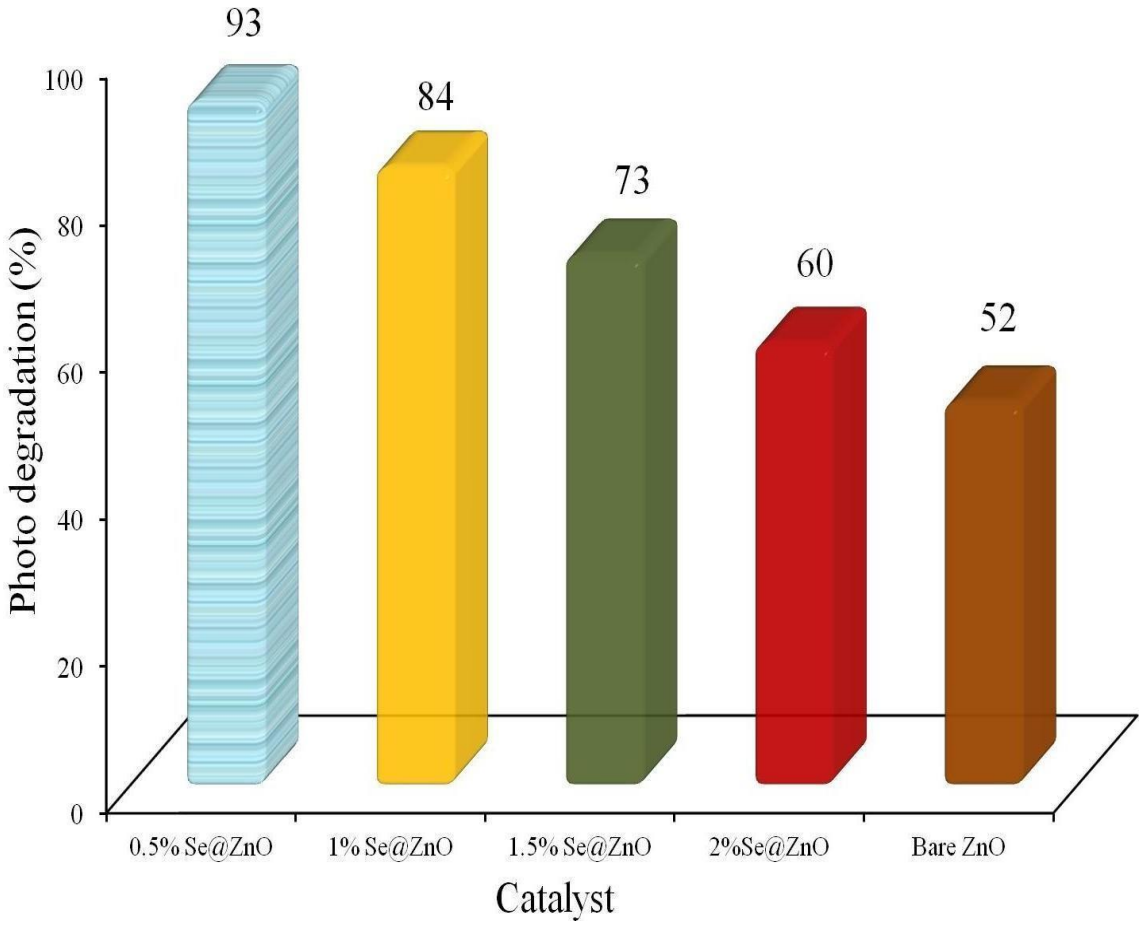

Fig. 26: Comparative photodegration efficiency of 4- Chloro guaiacol (50 ppm) by (0.5-2) wt% Se@ZnO photocatalyst under sunlight irradiation.

Further, the amount of CO_2 evolved by different (0.5-2) wt% Se@ZnO photocatalyst at the end of photo degradation process have been evaluated and demonstrated in figure 27. It was observed that nearly 88% of CO_2 evolved when 0.5 wt% Se@ZnO was used for degradation process.

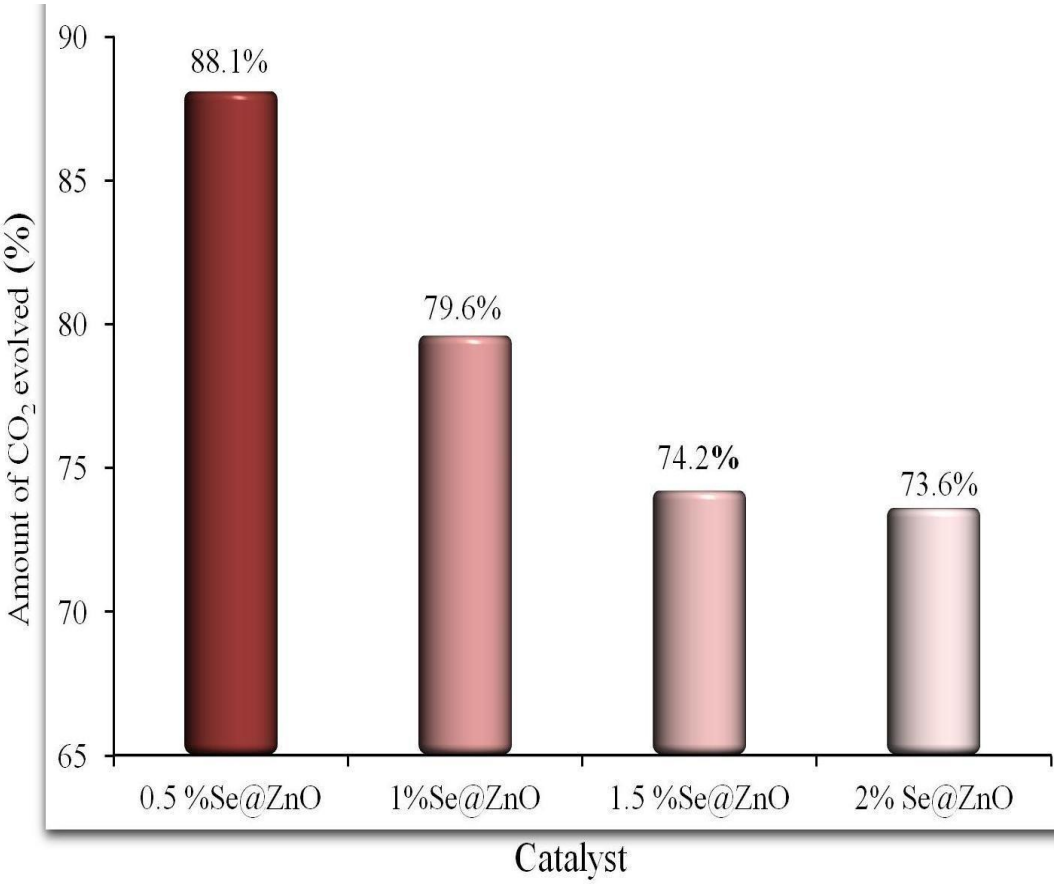

Fig. 27: Comparative CO_2 formation using different (0.5-2) wt% Se@ZnO photocatalysts under sunlight irradiation for 4-Chloro guaiacol.

Finally, to assess the efficiency of the prepared Se@ZnO photocatalyst a real life pharmaceutical effluent was degraded as shown in figure 28. It was observed that the COD level decrease from 1050 mgL^{-} **to 500 mgL^{-1} indicating that nearly 50% of the effluent was degraded after 240 minutes of sunlight irradiation**.

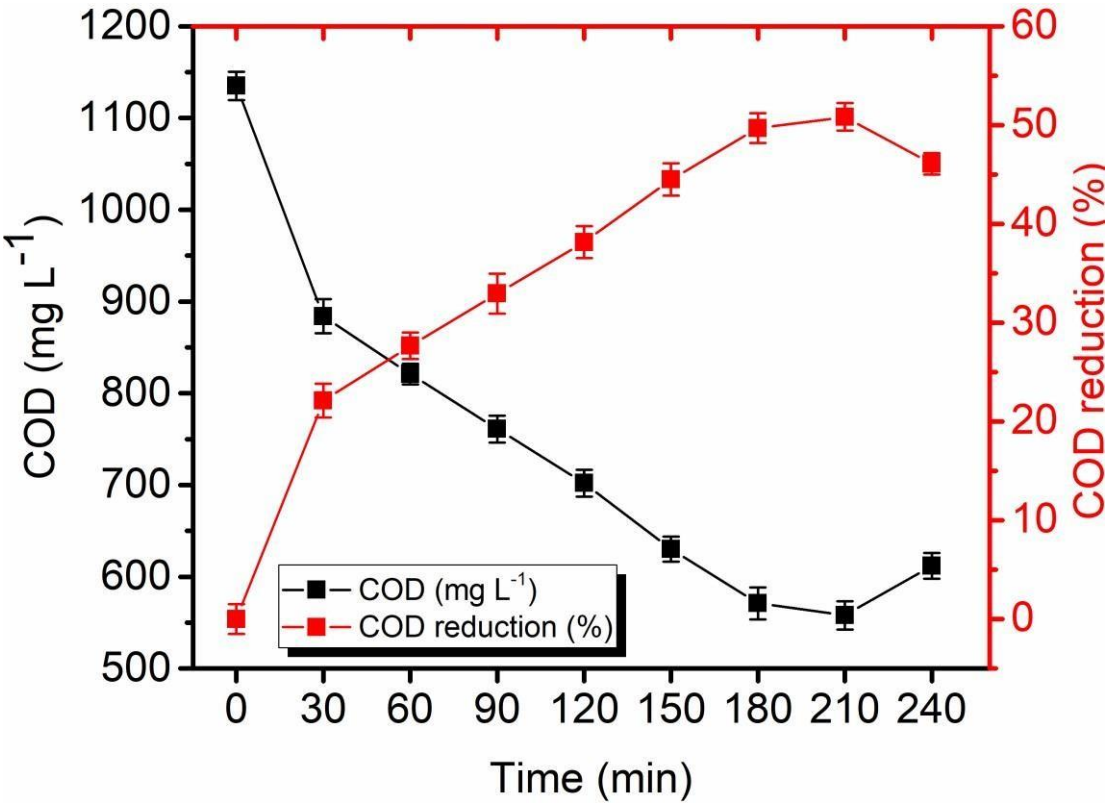

Fig. 28: Amount of COD reduction for real life pharmaceutical effluent after 240 minute sunlight irradiation with 0.5wt%Se@ZnO photocatalyst.

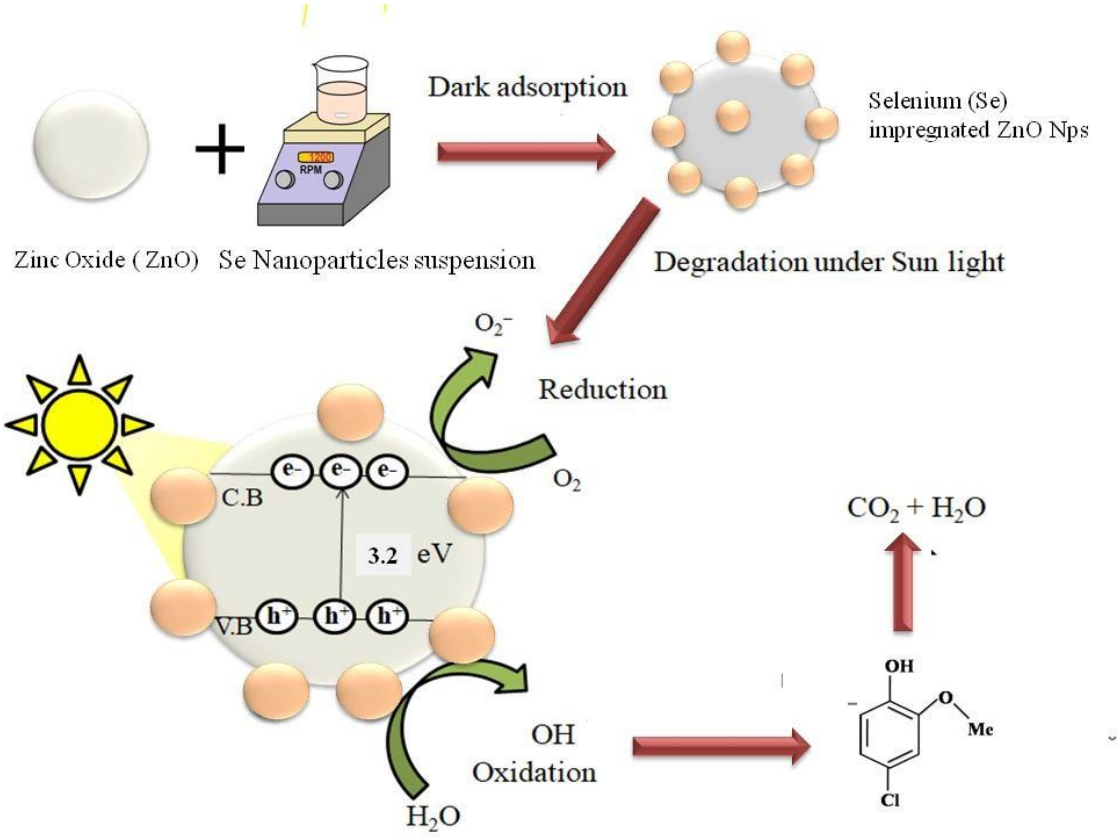

Scheme 3: Mechanism of adsorption and degradation of 4-Chloroguaiacol

5. Conclusion

The Biogenic Se NPs are successfully utilized as co-catalyst for increasing the photocatalytic activity of Se@ZnO. Various concentration of Se (0.5wt% to 2.0wt%) was impregnated on ZnO semiconductor using wet impregnation method which results in enhanced photocatalytic activity as compared to bare ZnO. Photocatalytic treatment involving these modified semiconductors suggests utilization of green technology for the elimination/degradation of highly toxic contaminants eluted out from industries as well as remediation of real industrial effluents. This method was observed to be more effective than the conventional method as during photocatalysis contaminant breaks down gradually, without any of its remains left behind. Also, problems of sludge generation and its disposal in landfills are not of concern when photocatalysis is involved. The catalyst itself remains unaltered after the degradation process and also do not require any additional chemical for the performance. Therefore, it results in cost effective simple operation methods for the remediation of pollutants. As photocatalysis is a surface phenomenon, contaminant gets associated with the catalyst; hence the process can occur even at low catalyst concentrations. Kinetic studies were performed for the degradation of 4- Chloroguaiacol using Se@ZnO and it was observed to follow first-order reaction kinetics where 50 mg of 0.5wt% Se@ZnO exhibits maximum degradation of 93% in 90 min under solar irradiations having k value ($2.9*10^{-2}$ min^{-1}). Real pharmaceutical industrial effluent was also subjected to the photocatalyst treatment using synthesized catalyst and significant reduction in COD value was observed. This significant activity of catalyst is due to impregnation of Se providing more electron and hole trapping sites preventing their recombination and resulting in generation of more e^--h^+ pair and enhanced formation of reactive oxygen species responsible for eliminating the pollutants. Evolution of 88% of CO_2 under solar radiations further confirms the complete mineralization of recalcitrant compound 4-chloroguaiacol.

6. References

1. McConnell, W. P.; Novak, J. P.; Brousseau, L. C.; Fuierer, R. R.; Tenent, R. C.; Feldheim, D. L., Electronic and optical properties of chemically modified metal nanoparticles and molecularly bridged nanoparticle arrays. ACS Publications: 2000.

2. (a) Sahoo, S.; Parveen, S.; Panda, J., The present and future of nanotechnology in human health care. *Nanomedicine: Nanotechnology, Biology and Medicine* **2007,** *3* (1), 20-31; (b) Doria, G.; Conde, J.; Veigas, B.; Giestas, L.; Almeida, C.; Assunção, M.; Rosa, J.; Baptista, P. V., Noble metal nanoparticles for biosensing applications. *Sensors* **2012,** *12* (2), 1657-1687.

3. Ananda, S., Synthesis and characterization of se-doped ZnO nanoparticles by electrochemical method: Photodegradation kinetics of indigo carmine dye and study of antimicrobial, antimitotic activities of se-doped ZNO nanoparticles. *American Chemical Science Journal* **2014,** *4* (5), 616-637.

4. Chen, Y.; Bagnall, D.; Koh, H.-j.; Park, K.-t.; Hiraga, K.; Zhu, Z.; Yao, T., Plasma assisted molecular beam epitaxy of ZnO on c-plane sapphire: Growth and characterization. *Journal of Applied Physics* **1998,** *84* (7), 3912-3918.

5. Reynolds, D.; Look, D. C.; Jogai, B.; Litton, C.; Cantwell, G.; Harsch, W., Valence-band ordering in ZnO. *Physical Review B* **1999,** *60* (4), 2340.

6. Kılıç, M.; Çınar, Z., A quantum mechanical approach to TiO2 photocatalysis. *Journal of Advanced Oxidation Technologies* **2009,** *12* (1), 37-46.

7. (a) Yan, S.; Wang, H.; Zhang, Y.; Li, S.; Xiao, Z., Direct solution-phase synthesis of Se submicrotubes using Se powder as selenium source. *Materials Chemistry and Physics* **2009,** *114* (1), 300-303; (b) Mondal, K.; Roy, P.; Srivastava, S. K., Facile biomolecule-assisted hydrothermal synthesis of trigonal selenium microrods. *Crystal Growth and Design* **2008,** *8* (5), 1580-1584.

8. (a) Chiou, Y.-D.; Hsu, Y.-J., Room-temperature synthesis of single-crystalline Se nanorods with remarkable photocatalytic properties. *Applied Catalysis B: Environmental* **2011,** *105* (1-2), 211-219; (b) Yang, L.; Shen, Y.; Xie, A.; Liang, J.; Zhang, B., Synthesis of Se nanoparticles by using TSA ion and its photocatalytic application for decolorization of cango red under UV irradiation. *Materials Research Bulletin* **2008,** *43* (3), 572-582.

9. Nath, S.; Ghosh, S. K.; Panigahi, S.; Thundat, T.; Pal, T., Synthesis of selenium nanoparticle and its photocatalytic application for decolorization of methylene blue under UV irradiation. *Langmuir* **2004,** *20* (18), 7880-7883.

10. Jain, R.; Gonzalez-Gil, G.; Singh, V.; Van Hullebusch, E.; Farges, F.; Lens, P., Biogenic selenium nanoparticles: production, characterization and challenges. *Nanobiotechnology, Studium Press LLC, USA* **2014**, 361-390.

11. Rajalakshmi, M.; Arora, A., Optical properties of selenium nanoparticles dispersed in polymer. *Solid state communications* **1999,** *110* (2), 75-80.

12. Kessi, J.; Ramuz, M.; Wehrli, E.; Spycher, M.; Bachofen, R., Reduction of selenite and detoxification of elemental selenium by the Phototrophic BacteriumRhodospirillum rubrum. *Applied and environmental microbiology* **1999,** *65* (11), 4734-4740.

13. Dhanjal, S.; Cameotra, S. S., Aerobic biogenesis of selenium nanospheres by Bacillus cereus isolated from coalmine soil. *Microbial cell factories* **2010,** *9* (1), 52.

14. Shah, M.; Fawcett, D.; Sharma, S.; Tripathy, S. K.; Poinern, G. E. J., Green synthesis of metallic nanoparticles via biological entities. *Materials* **2015,** *8* (11), 7278-7308.

15. Makarov, V.; Love, A.; Sinitsyna, O.; Makarova, S.; Yaminsky, I.; Taliansky, M.; Kalinina, N., "Green" nanotechnologies: synthesis of metal nanoparticles using plants. *Acta Naturae (англоязычная версия)* **2014,** *6* (1 (20)).

16. Thenmozhi, M.; Kannabiran, K.; Kumar, R.; Khanna, V. G., Antifungal activity of Streptomyces sp. VITSTK7 and its synthesized Ag2O/Ag nanoparticles against medically important Aspergillus pathogens. *Journal de Mycologie Médicale/Journal of Medical Mycology* **2013,** *23* (2), 97-103.

17. Ahluwalia, S.; Prakash, N. T.; Prakash, R.; Pal, B., Improved degradation of methyl orange dye using bio-co-catalyst Se nanoparticles impregnated ZnS photocatalyst under UV irradiation. *Chemical Engineering Journal* **2016,** *306*, 1041-1048.

18. Sastry, M.; Ahmad, A.; Khan, M. I.; Kumar, R., Microbial nanoparticle production. *Nanotechnology'(Wiley-VCH, 2004)* **2004**.

19. Kringstad, K. P.; Lindström, K., Spent liquors from pulp bleaching. *Environmental science & technology* **1984,** *18* (8), 236A-248A.

20. Tam, D.; Varhanickova, D.; Shiu, W. Y.; Mackay, D., Aqueous solubility of chloroguaiacols. *Journal of Chemical and Engineering Data* **1994,** *39* (1), 83-86.

21. Tan, I.; Ahmad, A.; Hameed, B., Adsorption isotherms, kinetics, thermodynamics and desorption studies of 2, 4, 6-trichlorophenol on oil palm empty fruit bunch-based activated carbon. *Journal of Hazardous Materials* **2009,** *164* (2-3), 473-482.

22. Levesque, M.; Vendette, E., Selenium determination in soil and plant materials. *Canadian Journal of Soil Science* **1971,** *51* (1), 85-93.

23. Association, A. P. H.; Association, A. W. W., *Standard methods for the examination of water and wastewater*. American public health association: 1989.

24. Janotti, A.; Van de Walle, C. G., Fundamentals of zinc oxide as a semiconductor. *Reports on progress in physics* **2009,** *72* (12), 126501.

alisha final

ORIGINALITY REPORT

17%	7%	13%	6%
SIMILARITY INDEX	INTERNET SOURCES	PUBLICATIONS	STUDENT PAPERS

PRIMARY SOURCES

1	Saniya Ahluwalia, N. Tejo Prakash, Ranjana Prakash, Bonamali Pal. "Improved degradation of methyl orange dye using bio-co-catalyst Se nanoparticles impregnated ZnS photocatalyst under UV irradiation", Chemical Engineering Journal, 2016 Publication	4%
2	Sakshi Bhardwaj, Bonamali Pal. "Photodeposition of Ag and Cu binary co-catalyst onto TiO 2 for improved optical and photocatalytic degradation properties", Advanced Powder Technology, 2018 Publication	2%
3	Nishant Srivastava, Mausumi Mukhopadhyay. "Biosynthesis and structural characterization of selenium nanoparticles mediated by Zooglea ramigera", Powder Technology, 2013 Publication	1%
4	Kian Mun Lee, Chin Wei Lai, Koh Sing Ngai, Joon Ching Juan. "Recent developments of zinc oxide based photocatalyst in water	1%

Alisha